UNIVERSITY OF CALIFORNIA SAN DIEGO

“Developing an Anti-FZD7 scFv for Lipid Nanoparticle based Drug Delivery”

A Thesis submitted in partial satisfaction of the requirements for the degree Master of Science

in

Bioengineering

by

Neha Balaji

Committee In charge:

Professor Karl Willert
Professor Ester Kwon
Professor Adam Engler

2023

This Thesis of Neha Balaji is approved, and it is acceptable in quality and form for publication on microfilm and electronically.

University of California San Diego

2023

Table of Contents

List of Abbreviations

APC……...Adenomatous Polyposis Coli

AXIN……Axis Inhibition

GSK3□……..Glycogen Synthase Kinase 3 alpha

CK1α……Casein Kinase 1 alpha

FZD……Frizzled

LRP……..LDL Receptor Related Protein

DVL……...Dishevelled

ROR……RAR Related Orphan Receptor

RYK……Receptor like Tyrosine Kinase

PTK7……...Protein Tyrosine Kinase 7

DSPE-PEG 200……
1,2-distearoyl-sn-glycero-3-phosphoethanolamine-N-[carboxy(polyethylene glycol)-2000

PB……Piggyback

EF1……...Human Elongation Factor 1

PEI……Polyethelenimine

IMAC……...Immobilized Metal Affinity Chromatography

HP……...High Performance

TMB…….3,3',5,5'-Tetramethylbenzidine

TCF……..T-cell Factor

HRP……Horseradish Peroxidase

DSPC……..Distearoylphosphatidylcholine

DBCO…….Dibenzocyclooctyne

DiI……1,1'-Dioctadecyl-3,3,3',3'-Tetramethylindocarbocyanine Perchlorate

GFP……Green Fluorescent Protein

List of Figures

List of Tables

Acknowledgements

I would like to begin by thanking my advisor Dr Karl Willert who has contributed immensely to my scientific learning and to the success of this project. I would also like to thank Dr Ester Kwon for being my co-advisor and lending her expertise to this project. I also thank Yazmin Hernandez from the Kwon lab for helping out with the LNP conjugation.

I'm also grateful to my lab members for being a constant source of support, knowledge and advice. I would especially like to mention Naycari De Luna, Erin D Jeffs, Ashley Key, Meghana Krishnan, Hailey Rowe and Christina N Wu. I would not have been able to complete this thesis and make progress as a scientist without them. I would also like to thank Myan Do, Diana Gumber and Pooja Sonavane for laying down the foundation for my work with their research.

I am especially grateful to the amazing team of GAPSWell Associates with whom I had the privilege of learning, laughing and growing outside of my program and research and gaining invaluable skills to take care of my mental well-being throughout my graduate school journey. I am immensely grateful to my family and friends for supporting me through all the tough times. Lastly, I would like to thank the Bioengineering department at UC San Diego for providing me with necessary resources inside and outside of the classroom. I would like to mention Dr Adam Engler for not only being on my committee but also for being an amazing teacher and academic advisor

ABSTRACT OF THE THESIS

"Developing an Anti-FZD7 scFv for Lipid Nanoparticle based Cancer Drug Delivery"

by

Neha Balaji

Master of Science

University of California San Diego, 2023

Professor Karl Willert, Chair

Professor Ester Kwon, Co-Chair

The WNT signaling pathway plays an important role in embryonic development and adult tissue homeostasis. However, cancer cells often can use this pathway to acquire 'stem-cell like' properties aiding proliferation, self-renewal and chemoresistance[1]. Several therapies targeting the WNT pathway have been developed successfully, but owing to adverse side-effects, many of these have not advanced through clinical trials[1]. Further, the WNT pathway's pleiotropic nature and complexity across different cancer types, necessitates the development of precise and targeted therapies. Previous studies have found that the WNT receptor, Frizzled class receptor 7 (FZD7), shows elevated expression in several cancer

types, making it a potential target for cancer therapies[4]. Lipid nanoparticles (LNPs) have been used in targeted cancer therapies for the diversity of payloads they can accommodate and their enhanced permeability and retention in tumor vasculature[16]. Thus, I propose that LNP enclosed anti-cancer payloads can be specifically delivered to FZD7 expressing tumor cells with the help of a targeting molecule. To that end, I have engineered a FZD7 targeting Single Chain Variable Fragment (F7-scFv) and tested lipid nanoparticles conjugated with the F7-scFv for their ability to bind to cells in a receptor dependent manner, to potentially be used to deliver anticancer therapeutics to tumors.

CHAPTER 1: INTRODUCTION

1.1 The WNT Signaling pathway

1.1.1 The Role of WNT Signaling in Embryonic Development and Cancer

The WNT signaling pathway is a key process in regulating embryonic development and stemness. WNT, by interacting with its receptors, effectors and inhibitors controls embryonic cell fate, proliferation and apoptosis[1]. In the absence of WNT, β-catenin is phosphorylated by the destruction complex which consists of APC, AXIN, GSK3β and CK1α. β-catenin is then subsequently ubiquitinated and proteolytically degraded preventing it from translocating to the nucleus and turning on WNT target genes. When WNT is present, it binds to its receptors FZD and LRP 5/6 and triggers a cascade of events by which the destruction complex is inactivated by the protein DVL allowing for the cytosolic accumulation of β-catenin which is then able to translocate to the nucleus and interact with transcription factors to regulate expression of several target genes[2]. The normal functions of WNT in stem cells are often hijacked by cancer cells to allow cancer stem cells to self-renew, proliferate and acquire chemoresistance [3]. Dysregulation of the WNT signaling pathway in cancer happens through deregulation and mutation of several players which include APC, AXIN, β-catenin, WNT agonists and many more [4].

Mammals express 19 different WNT proteins that signal through a variety of cell surface receptors including FZD1-10, LRP5,6; ROR1,2; RYK, and PTK7[4]. Being a core component of WNT receptor complexes, FZDs are alluring pharmacological targets to disrupt the WNT signaling pathway in cancer. Previous studies mining publicly available data sets on The Cancer Genome Atlas (TCGA) have identified that FZD7 expression is

elevated in several solid cancer types in The Cancer Genome Atlas including breast and ovarian cancer (Figure 1.2 A)[4]. Additionally, increased FZD7 protein expression was observed in ovarian tumors compared with normal ovarian tissue (Figure 1.2 B). Thus, these studies indicate that FZD7 may be a tumor-specific antigen and a potential target for cancer therapeutics.

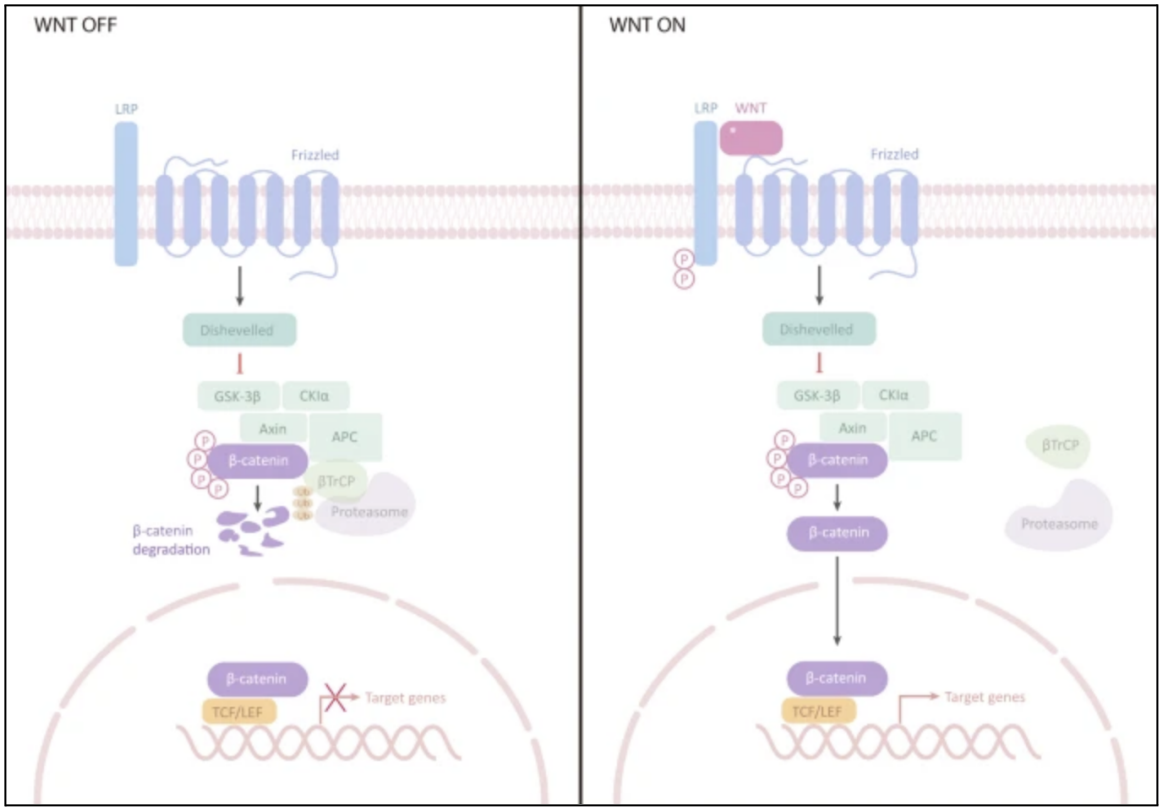

Figure 1.1: The WNT signaling pathway governs the expression of several genes triggering a cascade leading to the buildup and nuclear translocation of β-catenin which interacts with transcription factors TCF/LEF and turns on several genes during embryonic development [5].

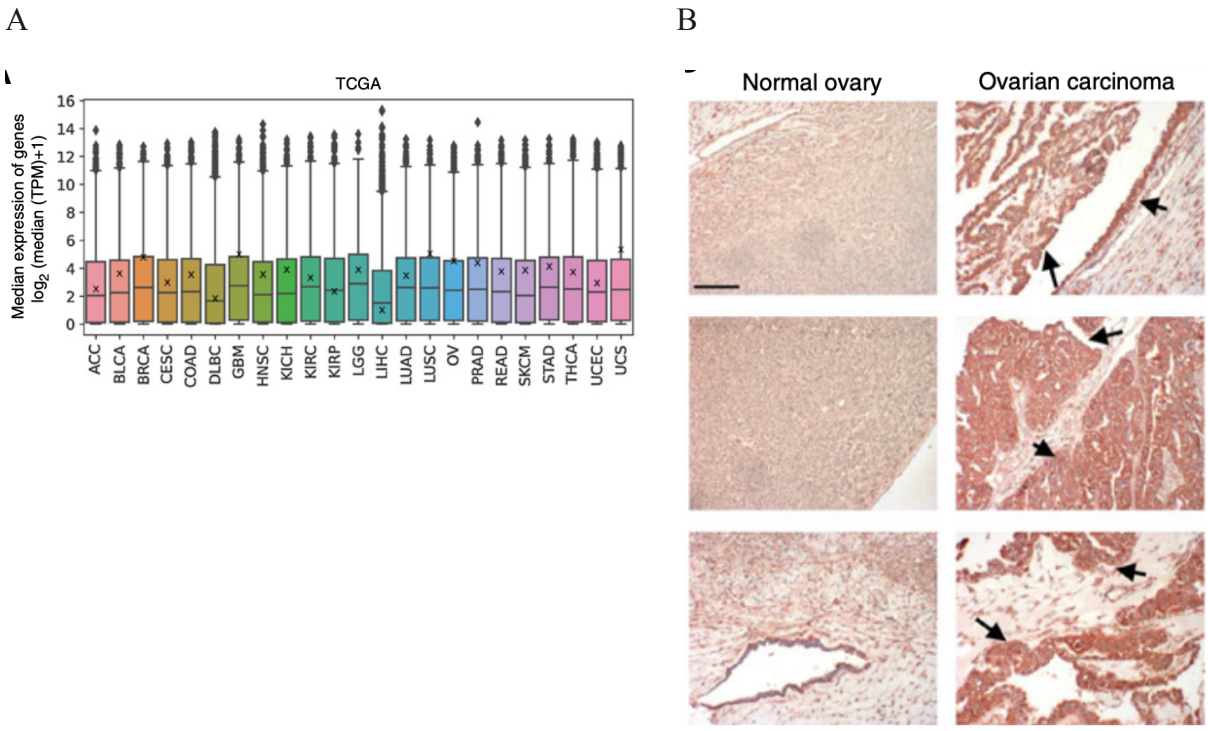

Figure 1.2: FZD7 expression is elevated in human cancers. (A) Median FZD7 expression in various cancer types by TCGA RNA-Seq data where the boxes represent 75% of all genes, the diamonds represent other individual genes outside this majority and the 'x' represents FZD7. BRCA (breast cancer), GBM (glioblastoma), LUSC (lung squamous cell carcinoma), OV(ovarian cancer), UCS (uterine carcinosarcoma) show elevated expression of FZD7. (B) Immunohistochemistry shows that FZD7 expression is low in normal ovaries and is elevated in ovarian carcinoma. Panels A and B were previously published in [4].

1.1.2 The Wnt Receptor- Frizzled (FZD)

FZDs are a part of the superfamily of cell surface receptors known as G-protein coupled receptors and are 7-pass transmembrane proteins. The N-terminus of FZD lies in the extracellular space and consists of a Cysteine rich domain (CRD) which is responsible for high affinity binding with the FZD ligand WNT, and a linker region. Together this encompasses the extracellular domain of FZD (ECD). Further, FZDs consist of a 7 pass hydrophobic transmembrane domain and a C-terminus intracellular domain. Our lab has previously developed a FZD7 targeting antibody (F7-Ab) whose binding epitope lies in the

extracellular linker region and maps to an 8 amino acid stretch that includes leucine at position 188 (L188). A detailed summary of the FZD7 targeting antibody is provided in section 1.4.1.

1.2 Antibody based Therapies for Cancer

1.2.1 Naked Antibodies

Antibody therapies have been actively engineered and developed for various diseases, including cancer, since the 1980's. Antibodies may produce their therapeutic effects in three ways: neutralization, antibody dependent cellular cytotoxicity (ADCC) and complement-dependent cytotoxicity (CDC). Neutralization occurs when antibodies bind to their target cell surface receptors in tumors and block the receptor-dependent signaling cascade which leads to loss of cellular functions, inhibition of proliferative activity and activation of pro-apoptotic pathways which eventually result in tumor regression[7]. ADCC is triggered when antibodies bind to their specific antigen on target cell surface via their variable fragment (Fv) and recruit immune cells, such as NK cells and macrophages (active immunity) or T-cells (passive immunity), which lyse and kill tumor cells. The CDC pathway comes into effect when the antigen-antibody complex binds to the C1 complex, triggering the complement cascade which leads to target cell lysis[7].

1.2.2 Antibody-Drug Conjugates (ADC)

An Antibody-drug conjugate consists of a monoclonal antibody bound to a chemotherapeutic drug through a chemical linker. The antibody component is designed to selectively bind to receptors found on the surface of cancer cells and release the cytotoxic drug upon endocytosis, thereby killing the cell[8]. 8 ADCs targeting different cancer cell surface markers have been approved by the FDA for clinical use in the US [8]. Our lab has previously been able to develop an ADC, Septuximab Vedotin which specifically binds to cell surface FZD7 and causes tumor regression in a murine ovarian cancer model[4].

1.2.3 Chimeric Antigen Receptor (CAR) Therapy

CARs are engineered receptors that redirect immune cells such as T cells and NK cells to recognize specific antigens and eliminate the cells expressing them. A CAR consists of four components 1) antigen binding domain 2) hinge region 3) transmembrane domain 4) one or more intra-cellular signaling domains[9]. While the antigen binding domain confers specificity to the CAR cells and helps them recognize the target antigen with its high binding affinity, the hinge region connects the binding domain to the transmembrane domain and provides flexibility, length and overcomes steric hindrance[9]. The transmembrane domain anchors the receptor to the cell membrane and is usually derived from natural proteins such as CD4, CD8α etc. The intra-cellular signaling domain is responsible for relaying signals to the interior of the cell post receptor-ligand interaction[9].

1.2.4 Antibody siRNA Conjugates (ARCs)

A major obstacle in RNA interference based therapies for cancer and other diseases is the low delivery efficiency and limited target organs. When conjugated with antibodies using covalent or non-covalent linkages, siRNAs can be selectively delivered to the target cell that over-express a certain antigen, owing to the high specificity of antigen-antibody reactions. Alnylam Pharmaceuticals has recently generated an ARC using their previously developed siRNA drugs which was successful in down regulating mRNA and protein expression of target genes in tumor cells. Many other pharmaceutical companies have also generated ARCs that have shown efficacy in achieving targeted interference effects [10].

1.2.5 Multispecific Antibodies

Cancer-signaling pathways are complex in that they involve multiple players to activate them and aid tumor cell proliferation. Monoclonal antibodies can thus be limited in their ability to downregulate these signaling pathways as they can target only one antigen at a time. To overcome this limitation, multispecific antibodies were developed to engage multiple cancer pathways or antigens and increase efficiency of targeted therapies. Multispecific antibodies may recruit immune cells (NK cells, T cells etc) to target tumors and eliminate them, bind to multiple closely spaced receptors to inhibit or activate their synergistic signaling pathways or target multiple tumor specific antigens to enhance tumor specificity [11]. Our lab has previously developed a bispecific antibody targeting FZD7 and its co-receptor LRP6 to act as a WNT mimetic and enhance WNT signaling in the absence of WNT[14].

1.2.6 Antibody Conjugated Nanoparticles (ACNPs)

Similar to ADCs, ACNPs use the specificity of antigen-antibody reactions to deliver drugs to target cells. They consist of an antibody specific to a tumor antigen conjugated with a nanoparticle which can encapsulate the drug payload to be delivered to the tumor cells. Nanoparticles offer the advantages of enhanced permeability and retention (EPR), controlled drug release, reduced off-target effects and high dose delivery. ACNPs are endocytosed by the target cell upon binding of the antibody component with its antigen, where the ACNP can deliver the drug by diffusion through the endosomal membrane or by lysosomal degradation [12].

1.3 Single Chain Variable Fragment (scFv)

Single chain variable fragments are a part of a larger class of non-Ig scaffold proteins. A scFv consists of a variable heavy chain (V_H) and variable light chain (V_L) joined by a flexible peptide linker. The weight of a scFv averages around 25 kDa which allows it to penetrate through tumors better and also prevent Fc related immunologic reactions, both advantages over immunoglobulins. Moreover, their small size allows for higher loading capacities, less surface and crowding and better orientation of targeting ligands, leading to overall improvements in efficacy [13].

1.4 FZD7 Targeting Antibody (F7-Ab)

Our lab has previously developed a FZD7 targeting antibody (F7-Ab) which is a chimeric human/mouse IgG1[14]. This antibody was derived from a bacterially produced antigen binding fragment (Fab) described by Fernandez et al., 2014[15]. This study showed that the FZD7-Fab does not recognize FZD1 and FZD2 which are the most similar to FZD7 of all the FZDs. By Flow cytometry, they also showed that the FZD7-Fab successfully binds to endogenously expressed FZD7.

1.4.1 Binding Epitope and specificity

Gumber et al.(2020) [14] characterized the F7-Ab by mapping the FZD7 binding site to the neck region between its cysteine rich domain (CRD) and its first transmembrane domain. F7-Ab epitope was mapped to an eight amino acid stretch containing L188 and protein alignment indicated that this neck region was the only extracellular portion containing differences between human FZD7 and mouse Fzd7 (disregarding the amino-terminal signal sequence). Further, a single amino acid change at position 188 from leucine to proline (P188) renders hFZD7 non-reactive to F7-Ab. More importantly, mutating the corresponding residue in mouse Fzd7, proline at position 188 to leucine renders mFzd7 reactive to F7-Ab. The F7-Ab was shown to be specific to FZD7 by ensuring absence of cross-reactivity with 9 other human FZDs (FZD1-6, 8-10). Since, the FZD7 targeting scFv is derived from the above described proteins, we speculated that it is specific to hFZD7 too.

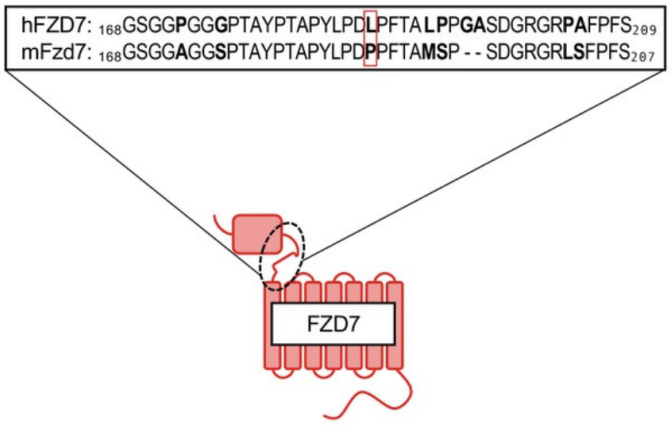

Figure 1.3: The amino acid sequence in the 'neck' region of FZD7 forms the binding epitope for F7-Ab. The red box indicates amino acid position 188 in hFZD7 and mFzd7 [14].

1.5 Lipid Nanoparticles (LNPs)

Lipid Nanoparticles are becoming increasingly common vehicles for delivering a wide range of therapeutics in the pharmaceutical industry. From the earliest and simplest liposomes to more complex lipid structures such as solid-lipid nanoparticles, nanostructured lipid carriers and cationic lipid–nucleic acid complexes, LNPs have presented several advantages leading to numerous clinical applications [16]. Liposomes have been used to encapsulate anticancer drugs exhibiting low solubility in water and increase their aqueous solubility. Doxil, one of the earliest liposomal nano-carriers of medicine, consists of a liposome (DSPE-PEG 2000) carrying the antitumor drug doxorubicin for the treatment of ovarian cancer [16]. LNPs have also helped make progress in nucleic acid delivery for gene therapies. Encapsulating gene therapy agents like mRNA

and siRNA in cationic lipid nanoparticles circumvents their poor diffusion across plasma membranes due to their overall negative charge and hydrophilicity [16].

Solid lipid nanoparticles (SLN) and nanostructured lipid carriers (NLC) are solid lipid and liquid lipid structures respectively which have several improvements than earlier generations of LNPs such as enhanced physical stability, higher loading capacity, higher bioavailability of drugs and more precise drug release [16]. SLNs and NLCs comprise lipids such as fatty acids, fatty alcohols and waxes and stabilizing agents such as surfactants. In addition, LNPs exhibit enhanced permeability and retentivity (EPR) in the context of cancer therapies. The defective and permeable vasculature of cancerous tumors allows LNPs to readily diffuse into the bloodstream and get lodged in the tumor microenvironment [12].

For my research project, I have developed a FZD7 targeting scFv (also referred to as F7-scFv throughout the paper) which specifically binds to FZD7, and conjugated it to LNPs in order to selectively bind and deliver drugs to FZD7 overexpressing tumor cells.

CHAPTER 2: MATERIALS AND METHODS

2.1 Generation of scFv Plasmid

The following strategy and steps were used to generate the scFv plasmid "F7 N-terminal (N)' 6xHis tag PB PuroR" (Plasmid 1).

1. Plasmid and Primer design: A FZD7 scFv plasmid was first designed electronically using Benchling's DNA/RNA sequence option. The plasmid sequence was largely borrowed from another plasmid in our lab's plasmid database, F7L6(Bp3)-Fc N 6xHis tag PB PuroR (Plasmid 2) which consisted of the following components going from N-terminal to C-terminal: an N-terminal signal sequence, an N-terminal 6xHis tag, FZD7 V_h, FZD V_l, LRP6 V_h, LRP6V_l, hIgG Fc. The plasmid also consisted of a CMV promoter for the gene of interest, Puromycin resistance gene (PuroR) with EF1 promoter, Ampicillin resistance gene (AmpR). The electronic file for the new plasmid consisted of the N-terminal signal sequence, N-terminal 6xHis tag, FZD7 $V_{h,}$ FZD V_l, borrowed from the previous plasmid. A single Cysteine (TGT) residue was added in between the 6xHis tag and the scFv sequence. The selectable markers (AmpR and PuroR) were also included in the new sequence. Due to the large size of the resultant plasmid (8038 bp) the sequence was amplified with 3 primer sets, one set for the gene of interest (insert) and two sets for the backbone. Primers were designed in order to add the Cysteine residue in the described spot and amplify the required regions of the template plasmid's backbone. This Cysteine is important for chemical conjugation of the scFv to LNPs.

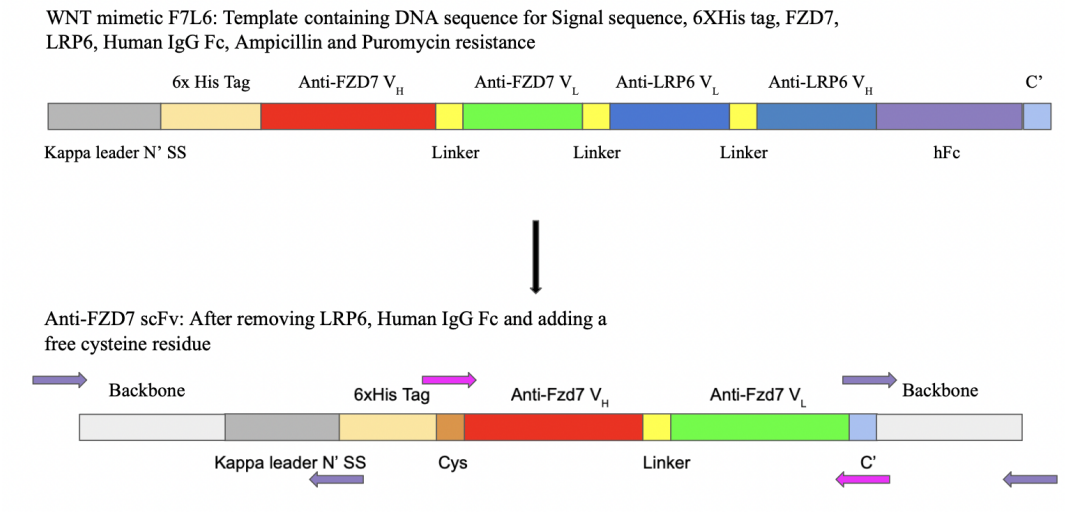

Figure 2.1: Schematic representation of the design of the plasmid containing gene of interest (Anti-FZD7 scFv). The pink and purple arrows on the bottom figure represent the annealing of primers required to synthesize the plasmid using the template (top figure).

Table 1: List of Primers used to amplify required regions of the template plasmid.

Oligo Name	Oligo Sequence	Application
Anti-FZD7 forward Sequencing Primer	CATCATCATCATCATCAT TGTGGAGAGGTCCAAC TGGTAGAGAGTGG	To amplify N-terminal signal sequence, N-terminal 6xHis tag, FZD7 $V_{h,}$ Linker, FZD Vl and insert Cys (TGT) between 6xHis tag and FZD7 V_h
Anti-FZD7 reverse Sequencing Primer	TTTGTCAGATCTAACCA TTTATTTGAGTTCCAAT TTCGTCCCTGCCC	To amplify N-terminal signal sequence, N-terminal 6xHis tag, FZD7 $V_{h,}$ Linker, FZD Vl and insert Cys (TGT) between 6xHis tag and FZD7 V_h
Plasmid 2 backbone forward sequencing primer 1	AAGGAATTTTGGTCATG AGATTATCAAAAAGGAT TCTTCAC	Backbone primer set 1
Plasmid 2 backbone reverse sequencing primer 2	ACAATGATGATGATGAT GATGGTCACCAGTGGA A	Backbone primer set 1
Plasmid 2 backbone forward sequencing primer 3	AGCTAGCGAATTCGAAT TTAAATCGGCCTC	Backbone primer set 2
Plasmid 2 backbone reverse sequencing primer 4	ATGGTTAGATCTGACAA AACTCACACATGCC	Backbone primer set 2

2. PCR Amplification and Gibson Assembly: The described 3 sets of primers were used to produce the desired sequence fragments in three separate PCR reactions which were verified by agarose gel electrophoresis. The desired DNA bands were gel extracted using the NEB Monarch DNA Gel Extraction kit and then Gibson assembled to generate the fully circular plasmid construct containing the required

sequences to produce the scFv of interest. The PCR and Gibson assembly reactions were set up as follows.

Table 2: PCR reaction components and volumes.

Component	Amount (µl)
Template DNA at 50 ng/ml (Plasmid 2)	1
Forward Primer (10 uM)	1
Reverse Primer (10 uM)	1
CloneAmp Mastermix	12.5
H_2O	9.5
	Total = 25 µl

Table 3: PCR Settings

PCR Step	Temperature (℃)	Duration (seconds)
Denaturing	98	10
Annealing	58	30
Extension	72	8

Gibson Assembly reaction: The gel extracted DNA fragments were added to the Gibson reaction mix in the ratio of 4:1:1 (Insert: backbone fragment 1:backbone fragment 2).

Table 4: Gibson assembly reaction components and volumes.

Components	Amount (µl)	pmoles/µl	Size (bp)
Insert DNA fragment	1	0.02915	745
Backbone fragment 1	1	0.0074	4914
Backbone fragment 2	1	0.0076	2634
Gibson Assembly mix	10		
H20	2		
	Total = 15 µl		

The above reaction mix was incubated at 50 ℃ for 15 minutes and immediately transformed into Top10 competent bacterial cells.

3. Bacterial transformation: One 100 µl aliquots of Top10 competent cells were taken out of -80 ℃ and thawed on ice. 5 µl of Gibson assembled plasmid was added to the thawed bacteria, mixed gently and incubated on ice for 30 minutes. The bacteria were heat shocked at 42 ℃ for 45 seconds and immediately transferred onto ice for 2 minutes to recover. The entire mixture was spread onto an LB agar plate with added ampicillin using glass beads and allowed to incubate overnight at 30 ℃.
4. Miniprep and Scale up of plasmid: Several prominent colonies were picked the next day and expanded in 4 ml LB broth with ampicillin and incubated overnight at 30 ℃. The plasmid DNA was then isolated using a homemade miniprep kit. Describe miniprep.
5. Verification by digestion and Agarose gel electrophoresis: The plasmid samples were digested using HindIII and SacII in the same fashion as described table 5.

Plasmid 1 was also digested in a similar manner as a positive control. The presence of 6xHis tag and Cys insert were verified by Sanger sequencing.

Table 5: Restriction digestion reaction components and volumes.

Component	Amount (µl)
Plasmid DNA (500 ug/ml)	1
HindIII	1
SacII	1
10X Buffer 2.1	2
H2O	15
	Total = 20 µl

6. Scale up of plasmid: 200 µl of the selected clone was inoculated into 200 ml of LB media with ampicillin and incubated overnight at 30 ℃. Promega Midi-prep kit was used to extract the plasmid and the purity and concentration of the final product were measured using a Thermo Scientific Nanodrop. The A260/A280 was ensured to be approximately 2 and the final concentration of plasmid was brought down to 1µg/µl.

2.2 Expression of scFv in Mammalian Cells

The following methods were followed in order to express the Anti-FZD7 scFv protein in mammalian cells and verify its expression. HEK 293 cells were cultured in DMEM media with 10% fetal bovine serum (FBS) and 1% Penicillin+Streptomycin (PenStrep). CHO cells were cultured in DMEM F12 media with 10% FBS and 1%

PenStrep. Henceforth, these will be referred to as HEK cells media and CHO cell media respectively.

1. Transient Transfection in HEK 293 cells: The Anti-FZD7 scFv protein was expressed in HEK 293 cells by transient transfection using a PEI to plasmid ratio of 1:4. HEK 293 cells were grown to 70% confluency in a 6 well plate. Two different amounts of the newly synthesized plasmid was transfected in addition to plasmid 2 as a positive control. The quantity of plasmids and PEI transfection agents are described in the table below.

Table 6: Transient transfection using PEI components and volumes

Plasmid	Concentration (µg/µl)	Desired Quantity for transfection (µl)	Volume of Plasmid DNA (µl)	Volume of PEI (µl)	Volume of OptiMEM (µl)
Plasmid 1	1	2	2	8	200
	1	3	3	12	200
Plasmid 2	1	2	2	8	200
Mock transfection	0	0	0	0	200

The above quantities of DNA were mixed with 200 µl of OptiMEM media in respectively labeled tubes. Both amounts of Plasmid 1 were set up in duplicates with plasmid 2 being the positive control and a mock transfection for negative control. PEI transfection agent was added to respective tubes in the volumes described above and the tubes were incubated at room temperature for 5 minutes. The cell media was aspirated and replaced with new HEK cell media in the

meantime. The DNA-PEI-OptiMEM mixtures were then added to the designated wells in a figure '8' pattern, gently swirled and returned to the incubator. The media was replaced by fresh HEK cell media the next day.

2. Stable transfection: CHO cells were stably transfected with both plasmid 1 and 2 using lipofectamine transfection agent and puromycin for drug selection. The transfection was performed using the thermo fisher Lipofectamine 3000 reagent. Parental CHO cells were plated on a 6 well plate and grown till 70% confluency in CHO cell media. The following steps were followed:

Table 7: Stable transfection using Lipofectamine

Steps	Procedure followed
Lipofectamine dilution	3.75 ul Lipofectamine 3000+125 ul OptiMEM (x3)
DNA dilution	1) scFv plasmid transfection: 1.5 ul plasmid 1 + 1ul transposase plasmid + 5 ul P3000 + 125 ul OptiMEM
	2) Positive control: 1.5 ul plasmid 2 + 1ul transposase plasmid + 5 ul P3000 + 125 ul OptiMEM
	3) Negative control (mock transfection): 5 ul P3000 + 125 ul OptiMEM

The diluted DNA was mixed with the diluted lipofectamine 3000 and incubated at room temperature for 15 minutes. Media on cells were aspirated and replaced with fresh CHO media in the meantime. The DNA+lipofectamine mixture was gradually

added to the designated wells, swirled gently and returned to the incubator. 48 hours post transfection, the cells were passed and resuspended in media with puromycin at 8 ug/ml (drug containing media). 3 10 cm plates were seeded as follows and kept under drug selection:

1% plate = 10 µl, 10% plate = 100 µl, 90% plate = ~900 µl. The same procedure was followed for the positive control cells and mock transfected cells.

3. Generating single cell colonies: When the 1% well of the scFv transfected cells reached confluence, cells were passed and resuspended in drug containing media. A 1:10 dilution of the cells was made and serially diluted on a 96 well plate in order to end up with one cell per well in the last row. To achieve that, 150 µl of drug media was added to each well of the first row of the 96 well plate and 200 µl was added to the remaining rows. 50 µl of diluted cells was added to each well of the first row and mixed well. 50 µl of this mixture was transferred to the next row and mixed well. The same was repeated till the last row of the 96 well plate. The plate was returned to the incubator and allowed to develop single cell colonies for about 3 weeks. Several single cell colonies were identified, expanded into a 24 well plate and tested for protein expression. Once the best clone was selected, it was further expanded into a 10 cm plate. Drug was added in all the expansion steps to maintain selective pressure.

2.3 Protein Collection

1. Collection of HEK 293 cell conditioned media (CM) and cell lysates (CL): Conditioned media was collected three days post transfection and filtered into 15 ml conical tubes using 0.22 μm syringe filters. In order to make cell lysates, cells were first washed with 1ml of PBS following which 100 μl of TNT lysis buffer was
2. added to each well of the 6 well plate till the cell began to peel off of the surface. The lysed cells were collected into separate Eppendorf tubes and centrifuged at 4 ℃ for 10 minutes at maximum speed. The supernatants were collected into newly labeled tubes. Both conditioned media and cell lysates for all samples were tested for protein expression.
3. Expansion and Collection of Conditioned media from Puromycin selected CHO cells: The 10 cm plate, seeded with the Puromycin selected clone was allowed to grow to confluence. The cells were split into 4 15 cm plates with 20 ml CHO cell media each, and a 10 cm plate for maintenance. Drug was added to all plates in this step. Upon reaching confluency, the conditioned media was collected from 15 cm plates and sterile filtered using 0.22 um vacuum filter. The cells from these 4 15 cm plates were further split into a total of 24 15 cm plates with 30 ml CHO cell media in each, without any drug added. 7 days post passage, the conditioned media was collected and filtered, and fresh media was added to the plates. Conditioned media was collected, filtered and replaced with fresh media every 5 days until the cells died. The entire expansion process starting from the 10 cm plate was repeated till

the desired volume of conditioned media was collected. Each batch of conditioned media was tested for protein expression.

2.4 Protein Detection and purification:

2.4.1 Western Blot

Protein expression was verified in transiently and stably transfected cells by Western blotting as described below. The same procedure was used to detect protein wherever mentioned.

1. Protein sample denaturation: 15 ul of CM and CL samples (HEK 293 or CHO cells) were mixed with 5 ul of 4x protein loading buffer. Samples were boiled for 5 minutes at 95 ℃.
2. Sample loading, SDS-PAGE and Transfer: 15 ul of each sample was loaded onto a SDS-Polyacrylamide gel and electrophoresis was performed at 220V for 45 minutes. After electrophoresis, the samples were transferred to a 0.22 um nitrocellulose membrane using a standard transfer box and transfer buffer.
3. Blocking and Antibody Hybridization: After the samples were transferred, the nitrocellulose membrane was thoroughly washed under running water and stained with Ponceau S stain to visualize protein bands and ensure the absence of air bubbles. The membrane was then washed with water and blocked with a blocking buffer (3% Non fat dry milk + 1% Bovine serum albumin in TBSt (20mM Tris Cl,150mM NaCl, 0.2% Tween 20)) for 1 hour at room temperature. Mouse Anti-6xHis tag antibody(primary antibody)

was diluted 1:2000 with fresh blocking buffer. After blocking, the membrane was incubated with the diluted primary antibody overnight at 4℃ while shaking. The blot was washed with TBSt 3 times for 5 minutes each. 1:20,000 diluted Anti-Mouse IgG HRP antibody (secondary antibody) was added to the washed membrane and incubated at room temperature for 45 minutes. The wash steps were repeated.

4. ECL Detection: 1ml of each substrate in the Super Signal West Pico Chemi Kit, Pierce was added to the washed blot and pipetted a few times to ensure full coverage. The nitrocellulose membrane was covered with cellophane wrap and taped to a photo cassette. The cassette was taken to the dark room where radiographic film was exposed to the blot for different amounts of time and developed using a film processing machine.

2.4.2 6xHis tag-Metal Ion Affinity Chromatography

After ensuring that the protein is expressed in the samples, the conditioned media was purified using a HiTrap IMAC HP column to isolate the His tagged Anti-FZD7 scFv. All chromatography techniques described in this paper were performed using the AKTA system. Described below is the procedure used to affinity purify scFv using a 1 ml HiTrap IMAC HP column for a 10 ml sample. Specifications about other column sizes and sample volumes will be mentioned in subsequent steps where necessary.

1. Charging the column with Ni^{+} ions: Before loading the column with the sample for metal ion based affinity purification, the column had to be charged with Ni^{+} ions. The column from Cytiva came pre-packed with a

sepharose resin with iminodiacetic acid (IDA) as the metal chelating molecule. The column was connected to the system and 2 ml of 0.2 M NiCl was loaded onto it using a 2 ml capillary loop and allowed to equilibrate. The column was then washed for about 2-3 column volumes (CV) with 1xPBS to remove any unbound Ni^{+} ions.

2. Method and settings: The column was equilibrated with the binding buffer till the UV reading was < 2 mAU (1xPBS+ 1-100 mM Imidazole, buffer A) for about 5CVs, followed by equilibration with elution buffer till the UV reading stabilized (1xPBS+ 500 mM Imidazole,buffer B) and buffer A again for about 5 CVs. 10 ml of CHO cell conditioned media was applied to the column using the 10 ml superloop injector and the flow through was collected in a 96 deep well plate. Linear gradient elution was carried out and the eluted protein was collected in 1 ml fractions in the same 96 deep well plate. The column was equilibrated with both buffer A and buffer B as described earlier, in order to wash off any contaminant proteins still present in the column. The input sample, flow through and eluent fractions were tested by western blot using the method described previously to ensure that the flow through is completely depleted of the protein and enriched in the eluent. Different imidazole concentrations were used with 1xPBS in the binding buffer in order to optimize the purification protocol. These were 50 mM, 60mM, 70mM, 80 mM and 100 mM.

2.4.3 Size Exclusion Chromatography

Size exclusion chromatography was employed to separate the scFv from other contaminant proteins after His tag affinity purification in the following manner.

1. Column Equilibration: Superdex 200 columns were used to separate proteins by size. The size and model of the columns are mentioned in the results section. The column was equilibrated with 1xPBS + 10mM β mercaptoethanol or other elution buffers mentioned wherever used, for at least 5CVs.
2. Sample application and Isocratic elution: Required amount of samples were loaded onto the column using either a capillary loop (for volumes <2ml) or superloops (for volumes > 2ml). Isocratic elution was performed over 1.5 CVs and the proteins were collected in deep well plates.

2.4.4 Ammonium Sulfate Precipitation

As an alternative to size exclusion chromatography, ammonium sulfate precipitation was explored as a strategy to separate proteins by size and also concentration the scFv as desired. In order to find out the salt concentrations at which both the scFv and the contaminant protein precipitate out, different concentrations of ammonium sulfate were tested on the same volume of affinity purified protein sample. Saturated ammonium sulfate (SAS) solution was made by dissolving 38 g of ammonium sulfate in 50 ml of water and the final volume of the solution was 71 ml. 75 ul of affinity purified scFv was added to 9 eppendorf tubes and labeled as 10%, 20%....90%. Required amount of SAS was added to each tube according to the chart provided by sigma. The tubes were mixed well and incubated at 4C for 1 hour. The precipitated proteins were pelleted by centrifuging the

tubes at 15,000 rpm for 10 min. The supernatant from each tube was collected and labeled while the pellets were resuspended in 37.5 ul. Both the pellets and supernatant for each salt concentration were tested by western blot.

2.5 Binding studies

The purified Anti-FZD7 scFv was tested for its binding activity to FZD7. The following experiments were carried out to show that the scFv successfully binds to FZD7.

1. **Protein G Sepharose Pulldown**: Since the Anti-FZD7 scFv structure is based on the original Anti-FZD7 antibody, we assumed that it binds to the linker in the extracellular domain (ECD) of human FZD7. Thus, a previously engineered FZD7 ECD-hIgG fusion protein was used to test its ability to bind to FZD7. FZD7 ECD-hIgG fusion protein was expressed in ExpiCHO cells, purified using a Protein A Sepharose column and verified by western blot. Four 15 ml conical tubes were labeled with the following conditions for the immunoprecipitation: 1) +scFv+ECD 2) +scFv-ECD 3) -scFv+ECD and 4) -scFv-ECD. 30 ul of each sample was put aside as 'input'. 10 ml of scFv conditioned media (+scFv) and unconditioned media (-scFv) were added to the respective tubes. 100 ul of purified ECD fusion protein was added to the +ECD tubes and the same amount of PBS was added to the -ECD tubes. The tubes were then rotated at 4 ℃ for an hour following which 40 ul of Protein G Sepharose bead slurry was added to each of the four tubes and rotated for an additional 1 hour. The tubes were then centrifuged for 5 minutes at maximum speed to help the beads settle down. The supernatant from each tube was collected and labeled as 'depleted fraction'. The beads were transferred to separate

Eppendorf tubes and washed 3 times with PBS to remove any nonspecifically bound proteins. The beads were then resuspended in 40 ul of 1X protein loading buffer and probed for scFv using the primary antibody: Mouse Monoclonal Anti-6xHis tag and Secondary Antibody:Anti-Mouse IgG HRP and for ECD using a secondary antibody only: Anti-Human IgG HRP. All other steps for western blot analysis were followed as described in section 2.4.

2. **Indirect ELISA**: An indirect ELISA was performed to test scFv binding activity as well as to quantify it after each purification step. Corning 96 well transparent half-area plates were used to perform the assay.

   Coating: After each purification step, the purified scFv sample was diluted 1:5, 1:25 and 1:125 and 50 ul of these samples were added to the plate in duplicates. To plot a calibration curve a FZD7 LRP6 single chain protein (detection protein) of known concentration was used. The detection protein was serially diluted 2X from 200 ug/ml to 1.56 ug/ml and 50 ul of each dilution was added to the plate in duplicates. PBS was added as blank. The samples were allowed to coat the wells overnight at 4 ℃.

   Washing and blocking: The wells were washed 5X with 150 ul PBSt (1X PBS + 0.05% Tween 20) and patted dry between each wash. The wells were blocked using 150 ul of blocking buffer (3% Nonfat dry milk+1%BSA in PBSt) for an hour at room temperature and washed again in a similar fashion.

Detection protein: 50 ul of 1:50 diluted FZD7 ECD hIgG fusion protein was added to each well and allowed to incubate for at least 1 hour at room temperature following which the wells were washed.

Antibody Hybridization: 150 ul of 1:20000 Anti-Human IgG HRP diluted in blocking buffer was added to each well and allowed to incubate for 1 hour at room temperature and washed.

Colourimetric detection and Standard curve : 75 ul of TMB substrate was added to each well and allowed to develop color for about 30 minutes. When the desired color was observed, 75 ul of stop solution was added and the absorbance was measured at 450 nm using a TECAN Infinite M200 pro plate reader. The absorbance values of standards and samples were pasted into the GraphPad Prism and Asymmetric Sigmoid 5PL model was used to analyze the data and extrapolate the concentrations of the samples.

Super TOP-Flash assay to study inhibitory effect on WNT Signaling: Previous studies with the Anti-FZD7 antibody in our lab have found that the binding of this antibody to its target FZD7 results in downregulation of WNT activity [15]. To see if this is true for the Anti-FZD7 scFv, a WNT reporter assay called Super TOP-Flash assay was performed to study its inhibitory effect on WNT signaling. For this activity assay, HEK 293 Super top flash cells which have been stably transfected with a plasmid containing the luciferase gene were used. This gene is controlled by the WNT target TCF promotor and hence can be used to measure and

compare WNT signaling between samples as a function of luminescence. The following steps were followed:

Day 0: Cells were seeded on a tissue culture grade 96 well plate at a seeding density of 10,000 cells per well.

Day 1: Cells were treated with the following treatments in triplicates and were incubated at 37 ℃ overnight:

1) No Wnt 3a +/- Purified scFv (1:100, 1:200 and 1:500)
2) 5nM Wnt 3a +/- Purified scFv (1:100, 1:200 and 1:500)
3) 5nM Wnt 3a +/- 100 ng/ml RSPO1 + Purified scFv (1:100, 1:200 and 1:500)

Day 2: Luciferase assay and cell titer glo assay were performed to measure Wnt activity and cell titer respectively.

1) Cell lysis: Cells were lysed with 45 ul cell lysis buffer (100mM K-PO_4 buffer, pH 7.8, 0.2% Triton X-100). The lysates were split into 2 opaque white plates with 20 ul of each sample and replicate.
2) Assay cocktail and luminescence measurements: 100 ul of the assay cocktail (0.25M Tris pH 7.8, 1M $MgSO_4$, 0.25 M ATP, 10 mM luciferin in H_2O), was added to each well of one plate and luminescence was immediately measured using the Promega plate reader and GloMax application. 100 ul of Promega cell titer glo reagent was added to the samples on the other plate and luminescence was measured similarly.

3) Normalizing values and plotting graphs: The luminescence reading from the luciferase assay was normalized to the cell titer glo value for each corresponding sample and plotted as bar graphs using Graphpad prism along with error bars.

2.6 LNP Synthesis and Conjugation with F7-scFv and F7-Ab

LNP synthesis and conjugation was done by the Kwon Lab, Department of Bioengineering at UC San Diego. The LNPs formulation used in this study is based on that described by Waggoner et al. 2023 [17], with some modifications introduced. Briefly, the LNP composition was MC-3:Cholesterol: DSPC: PEGylated Lipid: DiI at molar ratios of 50: 38.5: 10: 1.299: 0.2. MC-3 is an ionizable lipid which plays an important role in endosomal escape of cargo, DSPC is a phospholipid which acts as the helper lipid and Cholesterol and PEGylated lipid enhance the stability of the LNP [17]. DiI is a lipophilic red fluorescent dye used for lipid tracking. Additionally, linear GFP mRNA was encapsulated at a final concentration of 1.2 mg/ml into the LNPs to assess in vitro transcription following endosomal release.

Both the F7-scFv designed in this project and the F7-Ab previously developed by our lab were conjugated onto the LNPs. In order to conjugate the F7-scFv, maleimide-thiol chemistry was used utilizing the free cysteine introduced during plasmid design. Briefly, DBCO-Maleimide was incubated with the F7-scFv in a 5:1 ratio and rotated at room temperature. The DBCO labeled scFv was purified using a Zeba desalting column and incubated with the LNPs in a 1:25 molar ratio of LNPs:labeled scFv overnight at 4℃. The conjugated LNPs were then purified using a Nanosep 300k centrifugal filter. The F7-Ab

was conjugated to LNPs in a similar manner using Sulfo-NHS-DBCO for copper-free click chemistry[18].

2.7 In Vitro Targeting Studies

MA148 ovarian cancer cells were used to test LNP binding and uptake. Cells were plated onto a 24 well plate at a density of 30k cells per well and incubated at 37℃. The next day, the cells were treated with F7-scFv and F7-Ab conjugated LNPs diluted in RPMI media with 10% FBS and 1% PenStrep. Dosages of conjugated and unconjugated LNPs were determined based on the amount mRNA. For the first trial, MA148 wild type and FZD7 knockout cells were treated with 100 ul RPMI media with LNP-mRNA dosages starting from 5ug mRNA and serially diluted 5 times for subsequent dosages. After incubating the cells for 2 days, the media was aspirated off the cells and washed twice with PBS to remove unbound LNPs. The cells were imaged live using the EVOS M5000 microscope at 4X with the red fluorescent light bulb.

In order to optimize this experiment, further iterations were performed. MA148 wild type and FZD7 knockout cells were plated onto a 96 well plate at a seeding density of 6000 cells per well. After incubating overnight at 37℃, the cells were treated with LNP-mRNA dosages starting from 1ug and serially diluted 5 times for subsequent dosages. The next steps were performed as described above with any variations mentioned in the results section.

CHAPTER 3: RESULTS AND DISCUSSION

3.1 Generation of scFv Plasmid and protein expression:

The primers listed in Table 1 were used to amplify specific regions of the template plasmid. The size of amplicons were verified by agarose gel electrophoresis as shown below. The resultant fragments were of expected sizes.

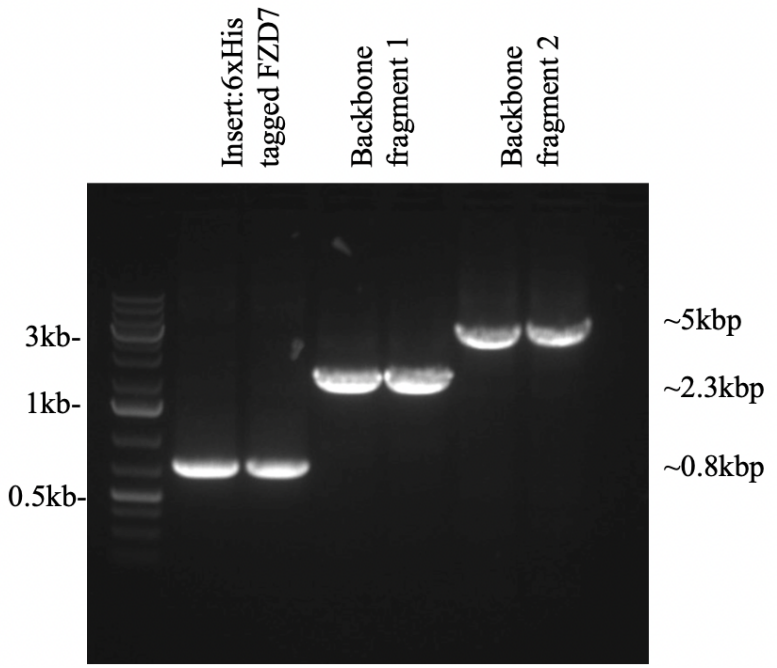

Figure 3.1: PCR Amplified DNA fragments were run on a 1% agarose gel and electrophoresis was performed at 120V for 25 minutes. The gel was imaged using a gel imager and bands were compared to a 1kb plus standard DNA ladder.

The above fragments were cut from the gel and purified using NEB Monarch Gel purification kit. Subsequently, Gibson assembly and bacterial transformation was performed as described in the methods section. Several clones were identified, their plasmid extracted and verified by digestion and sequencing.

A B

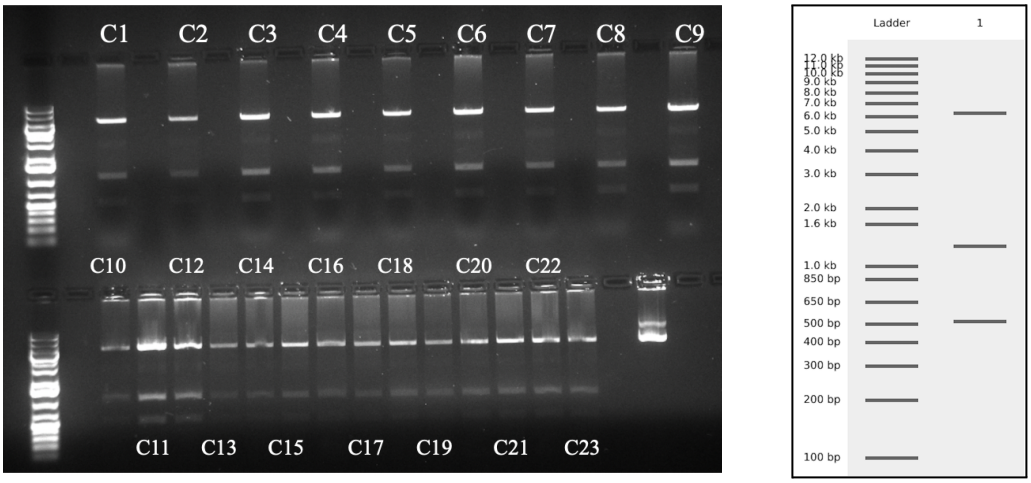

Figure 3.2: (A)Plasmid from all selected clones (C1-C23) were extracted using the Promega mini prep kit. The plasmid structures were verified by restriction digestion using HindIII and SacII and agarose gel electrophoresis. (B) A virtual digest was generated on benchling to visualize and compare the result of the restriction digest.

Clone 11 (C11) was selected to transiently transfect into HEK 293 cells to check protein expression. Protein expression was tested by western blot as described in the methods section. Mouse Anti-6xHis was used as the primary antibody and Anti-Mouse IgG HRP was used as the secondary antibody.

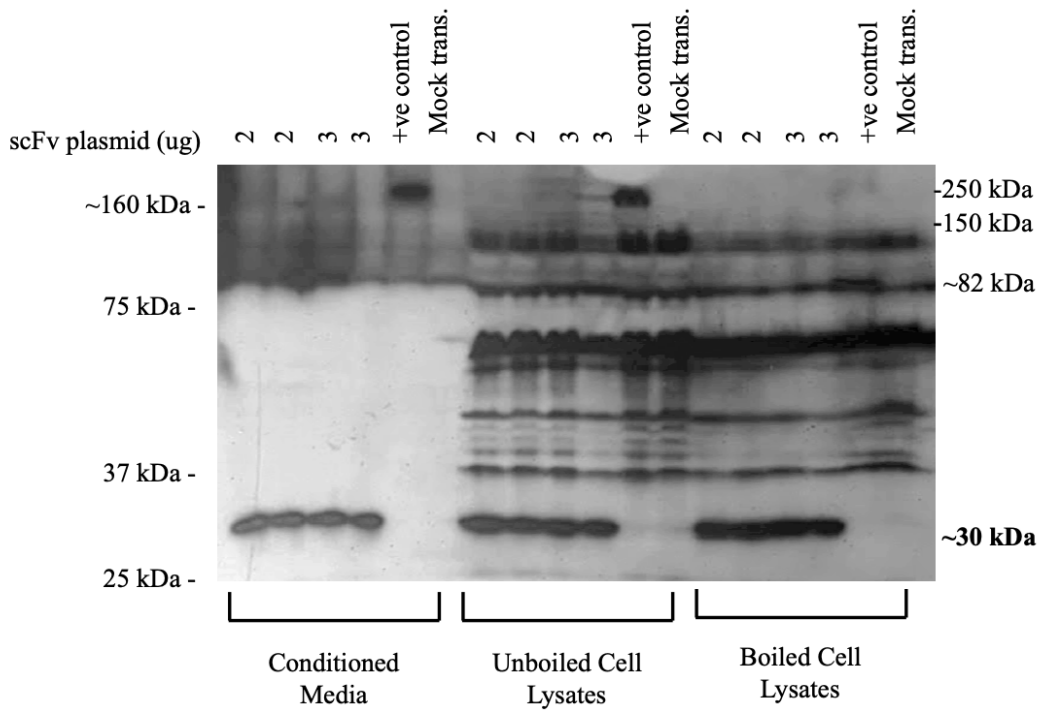

Figure 3.3: Conditioned media and cell lysate samples were tested using western blot with Anti-His tag antibody. All wells transfected with the scFv plasmid expressed the protein which is estimated to be about 30kDa. This is further confirmed with the absence of a band in mock transfected samples and the presence of the positive control band at ~160kDa in unboiled samples and ~82kDa in the boiled sample.

The plasmid containing the F7-scFv gene was then stably transfected in CHO cells and selected using Puromycin as described in the methods section. Serially diluted cells developed single cell clones in about 2 weeks out of which six were picked, expanded in 24 well plates and allowed to grow for another week. The conditioned media was collected from these clones and cells were lysed to verify protein expression using western blot.

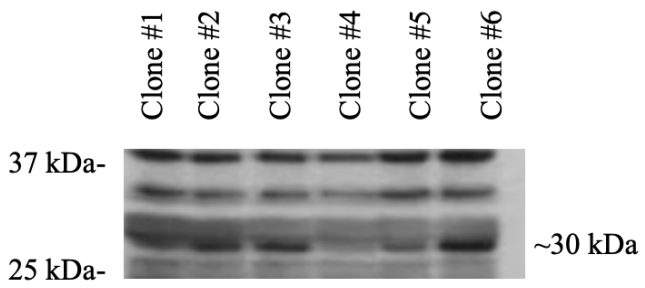

Figure 3.4: Six clones were picked and expanded after serial dilution. The Anti-His tag western blot revealed that clones 1,2,3,5 and 6 expressed the scFv. Clone 6 was selected for further studies.

3.2 FPLC Purification and troubleshooting:

10 ml of conditioned media was loaded onto a HiTrap IMAC 1 ml column charged with Ni ions. In order to find out the concentration of imidazole at which the protein is eluted and to optimize purification parameters, step elution was carried out. Buffer A was fixed at 50mM but the % buffer B was increased in a stepwise manner from 0% (50 mM) to 100% (500 mM) and the eluted protein was collected in 1 ml fractions in a 96 deep well plate. The protocol for step elution is shown below.

Table 8: Step elution protocol used to purify scFv conditioned media in order to optimize purification conditions.

% Elution Buffer	Imidazole Concentration (mM)	CVs
0	50	5
5	72.5	5
10	95	5
20	140	5
30	185	5
50	275	5
60	320	5
80	410	5
100	500	5

Step elution was performed using a binding buffer with 50mM Imidazole and an elution buffer of 500 mM Imidazole. The protein elutes at 20% of the elution buffer which is about 140 mM imidazole. However several concentrations of binding buffer were tested to confirm scFv binding and minimal binding of other contaminants to the column.

A

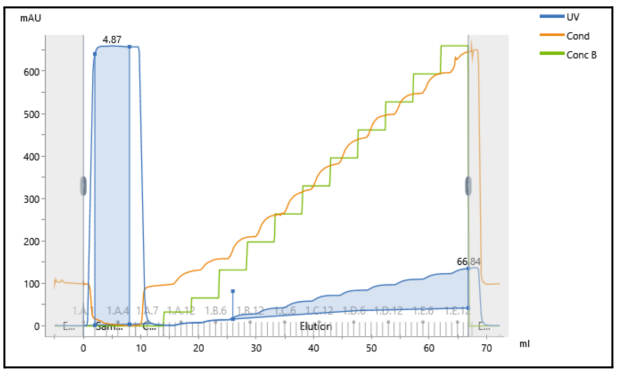

B

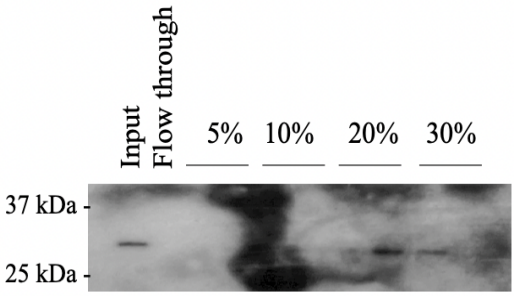

Figure 3.5: (A) Chromatogram showing the stepwise increase in concentration of imidazole (Conc B). The blue line shows UV absorbance of material passing through the column. UV peaks can be used to visualize proteins being eluted as they exhibit higher UV absorbance due to their aromatic amino acids. However other molecules such as imidazole also exhibit higher UV absorbance which necessitates further western blot investigation. (B) Step elution reveals that the scFv gets eluted at 20% imidazole concentration which is about 140mM.

A

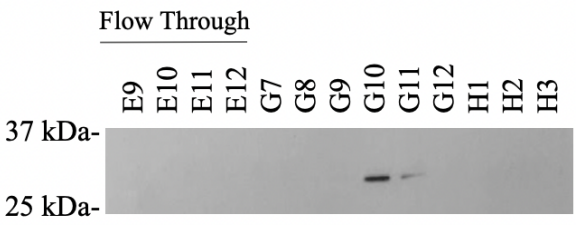

B

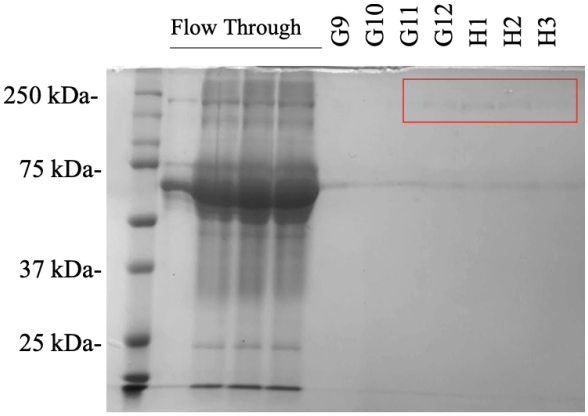

Figure 3.6: (A)Western blot shows that the protein is eluted in the expected fractions (input not loaded) at 50mM imidazole in the binding buffer. (B) Coomassie stained gel reveals the presence of a larger co-purified protein necessitating a secondary purification step.

A(i) A(ii)

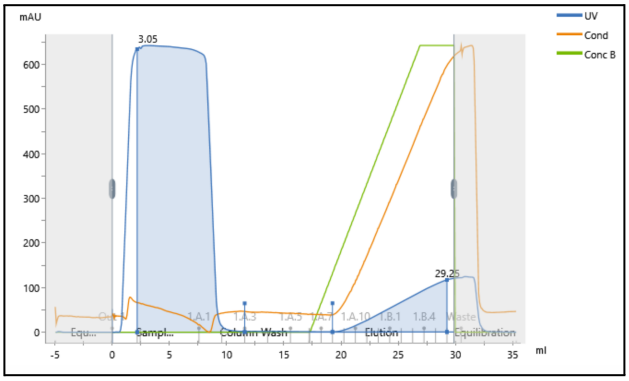

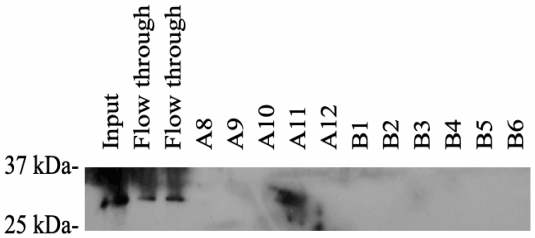

B(i) B(ii)

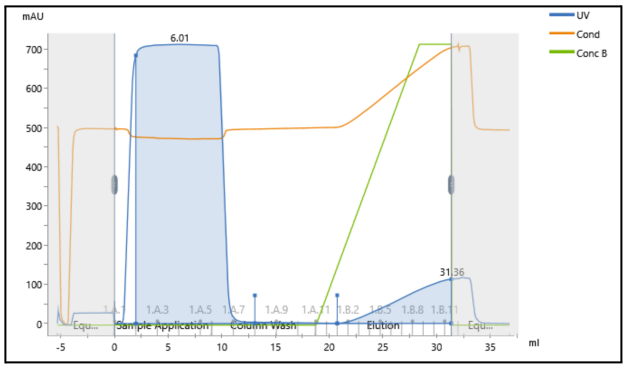

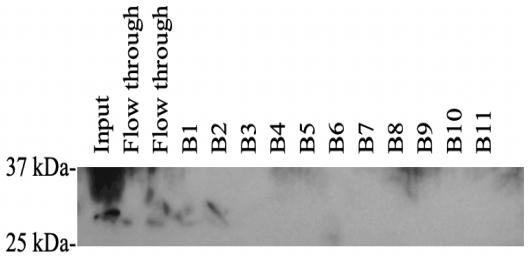

Figure 3.7: (A(i)) Chromatograms for an imidazole concentration of 80mM and (B(i)) 100mM show no discernable protein peak. (A(ii)) Western blots on sample from the indicated fractions of the 96 well plate at an imidazole concentration of 80mM and (B(ii)) 100mM in the binding buffer do not allow the protein of interest to bind to the affinity column's resin presumably due to the binding affinity of the protein being lower than the above concentration of imidazole.

My experiments show that imidazole concentrations of greater than 50mM does not allow the protein to bind to the Ni^{+} column and may be assumed to be displaced by imidazole. 60 and 70mM also yielded similarly unfavorable results. Thus, 50mM of imidazole was finalized for the binding buffer and the elution buffer was kept at 500mM. This, however necessitates another purification step to remove the contaminant protein shown in the Coomassie in fig. The next step was to scale up the purification in order to

obtain enough protein for LNP conjugation. 300 ml of CHO CM was loaded onto the same 1ml IMAC column and gradient elution was carried out. The eluent was collected in 1 ml fraction in a 96 deep well plate and the flow through was collected separately in 50 ml tubes. Protein enrichment in the eluent and depletion in the flow through was verified by western blot analysis. The 1 ml column was not able to completely deplete the protein from the input and enrich it in the eluent as bands corresponding to the input band are seen in the flow through fractions.

A

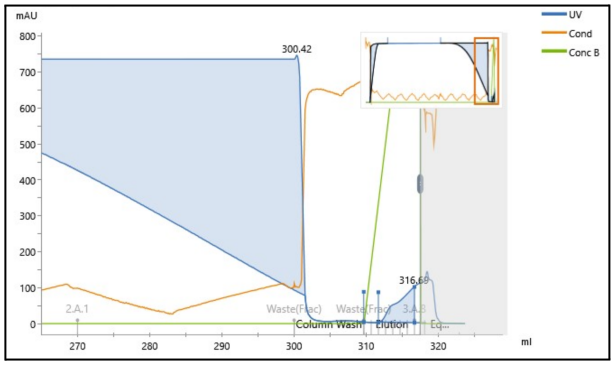

B

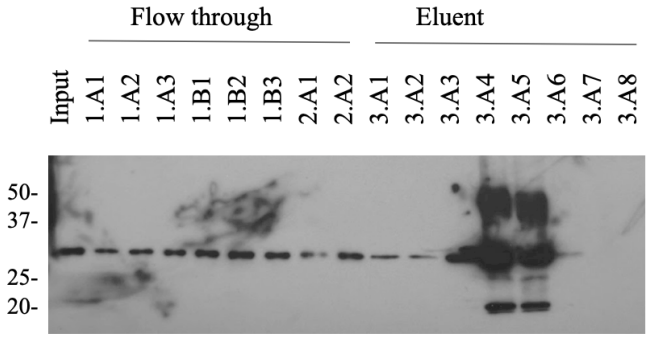

Figure 3.8: 300 ml of scFv conditioned media was purified over a 1 ml Hi-Trap IMAC column to assess the column's binding volume. (A) Chromatogram showing variations in UV absorbance as the input passes through the column. A small peak is seen in fractions 3.A3-3.A5 which is presumably where the scFv gets eluted. (B) The protein is eluted in the expected fractions. However, this western blot reveals that this column is insufficient to purify such large amounts as strong bands are seen in the flow through fractions.

In order to find out the degree to which the purification needs to be scaled up, the purified F7-scFv from a 10 ml affinity run was compared to another purified protein. This protein of known concentration was serially diluted 2 fold from 84 ug/ml. Western blot was performed on the different dilutions of the known protein and the purified scFv sample. The western shows that the scFv obtained from 10 ml CM is roughly the same as the 2.625 ug/ml known protein sample. From this, it was inferred that 4L of conditioned media will be required in order to purify about 1 mg of the F7-scFv.

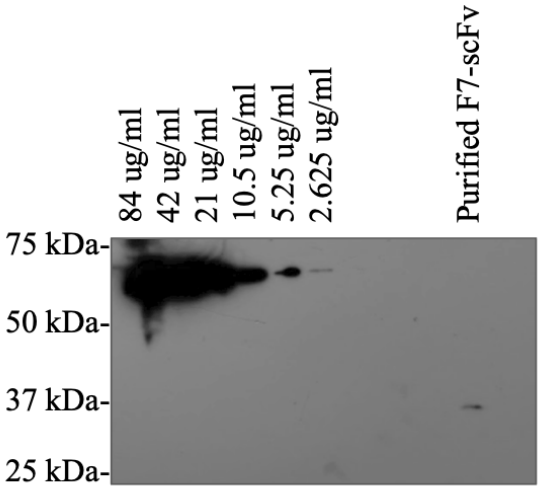

Figure 3.9: F7-scFv purified from 10 ml CM was compared to a protein of known concentration. Western blot revealed that the scFv obtained from 10 ml CM is roughly equal to 2.625 ug/ml. Thus in order to obtain 1 mg of protein, 4L of CM needs to be collected and purified.

Thus in order to scale up protein production, purification was repeated with a 5 ml HiTrap IMAC column charged with Ni^{+} ions. 500 ml of CHO CM was loaded onto the column and gradient elution was carried out. Eluent was collected in 1 ml fractions in a 96 deep well plate and the flow through was collected separately in 50 ml conical tubes. Western blot analysis of the fraction showed that the 5 ml column is better at depleting the

protein from the input sample and enriching it in the eluent. However, the last flow through fraction showed a band from which we concluded that a 5 ml column may still not be sufficient to deplete the protein from samples > 500 ml.

A

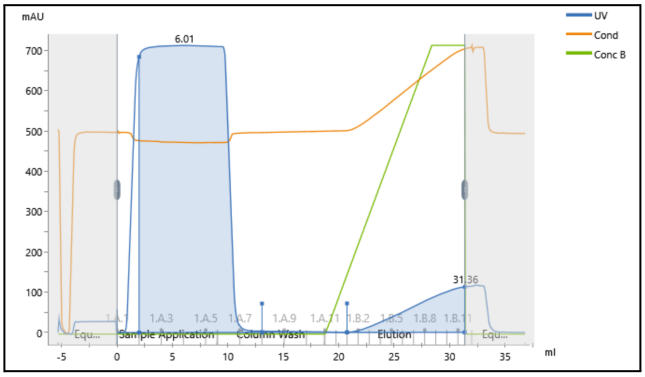

B

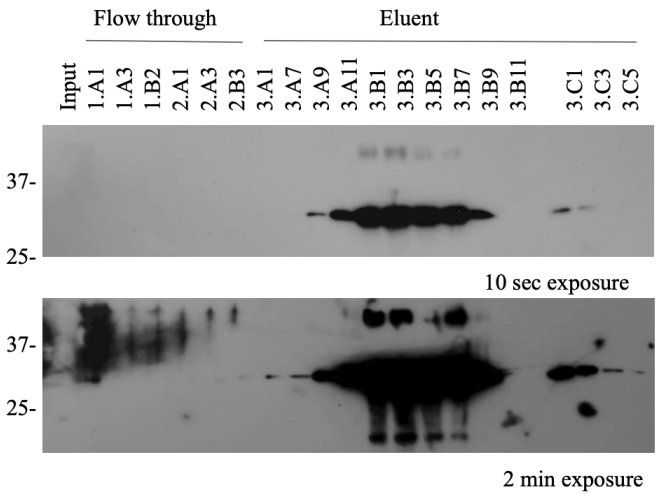

Figure 3.10: 500 ml of scFv conditioned media was purified over a 5 ml HiTrap IMAC column charged with Ni^{+} ions. The western blot revealed that this column is much better at purifying larger volumes. However, it may not be effective for volumes >500ml as the protein begins to appear in the final flow through fractions (2.A3, 2.B3) in longer exposures. Protein aggregation is seen at high concentrations (3.B1-3.B7) presumably due to intramolecular disulphide bonding between the free Cys residues.

Thus, we decided to perform the purification in a larger column. We purchased chelating sepharose fast flow 50ml resin and gravity packed it into a sufficiently large

column. The final column volume was calculated to be about 52 ml. The column was thoroughly washed with water to eliminate any ethanol after which it was equilibrated with the binding buffer. 4 L of F7-scFv conditioned media with 50mM Imidazole was loaded onto the column using the sample pump and gradient elution was carried out to collect the eluent in 2 ml fractions in a 96 deep well plate. Additionally, 10 mM of □-Mercaptoethanol was added to both the binding and elution buffers to prevent intramolecular disulphide bonds between the free Cys residues. The flow through was collected separately through the outlet valve. The western blot analysis of the input material, flow through and eluent fractions revealed that the 52 ml column was successful in completely depleting the scFv from the input sample and enriching it in the eluent.

A

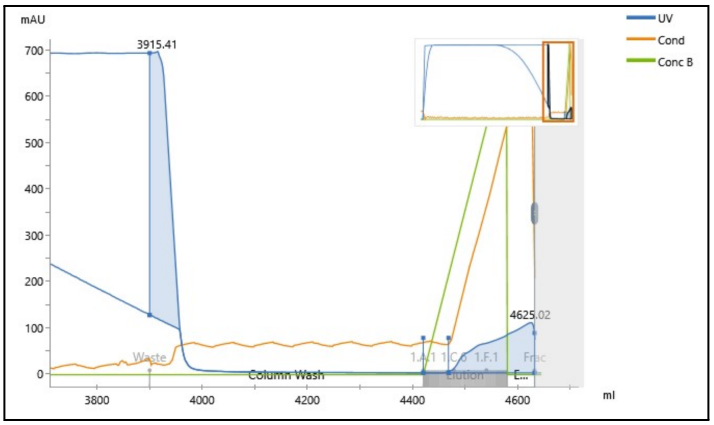

C

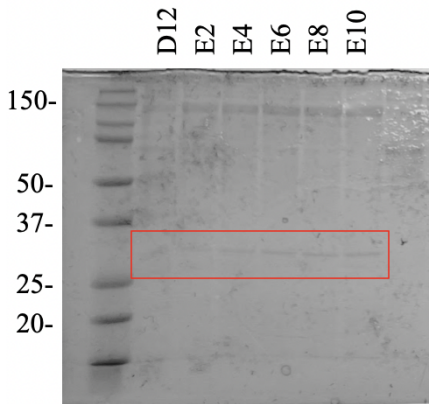

B

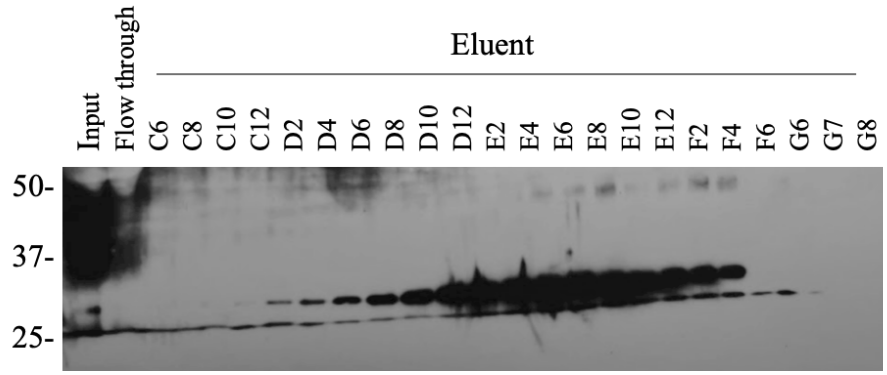

Figure 3.11: (A) The chromatogram shows slight variations in UV absorption between fractions C9-F4. (B) Western blot shows that the 50 ml column is able to fully deplete the scFv from the conditioned media and enrich it in fractions D4-F4. This is confirmed by the absence of a band corresponding to the size of scFv in the flow through. Additionally, the □-Mercaptoethanol aids in reducing protein aggregation at high concentrations as seen by the relatively the faint bands at ~50kDa. (C)Coomassie staining on the fractions showing highest protein signal confirms the elution of the scFv (highlighted in red). However, a larger co-purified contaminant at ~150 kDa is also observed.

Size exclusion chromatography was employed to remove the larger contaminant protein from the samples in order to make it cleaner. Before sizing the entire volume of the scFv, smaller volumes of the affinity purified sample were tested using a 10/300 Superdex 200 sizing column under different conditions. 200 ul of the affinity purified sample was loaded onto the 10/300 Superdex 200 and eluted either using only 1x PBS or 1x PBS +10mM □-Mercaptoethanol. As size exclusion chromatography separates proteins by their sizes where larger proteins eluting first, we expected the contaminant protein to eluted first and then the scFv. For each sizing run, several fractions corresponding to every UV peak were selected and verified by western blot. In both runs, the scFv was found in fractions corresponding to the second UV (indicated by black arrows in figure 3.12). This showed that the sizing column could be separating the two proteins.

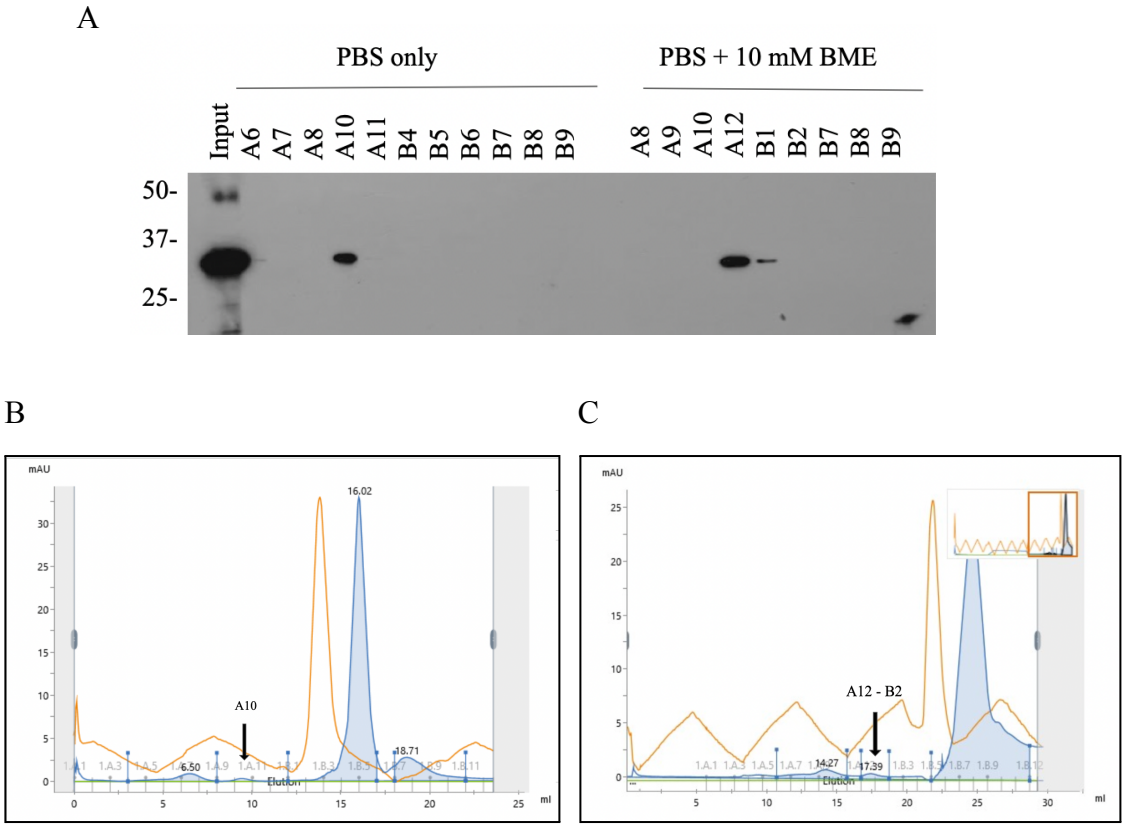

Figure 3.12: (A) Western blot on fractions corresponding to different peaks in both chromatograms shows that the scFv is eluted in fractions under the second UV peak when eluted only with PBS (B) or with PBS and BME (C). Further, no significant difference is seen in both conditions. The black arrows in the chromatogram show the peak and fractions where the scFv was found. This result shows that the size exclusion was successful in separating the larger protein (presumably eluted corresponding to the first UV peaks in both chromatograms) from the relatively smaller scFv.

Going by the above result, we decided to perform the size exclusion in PBS. To perform the size exclusion on a larger volume, the 26/60 Superose 200 column was used. After equilibrating with PBS, 8 ml of affinity purified sample was loaded onto this column and the eluted fractions were collected in 3 24 deep well plates where each fraction was 9 ml. Upon western blot analysis, it was found that the scFv was eluted in fractions corresponding to the first peak. To further confirm this, a Coomassie stain was done to

visualize the contaminant protein which was found in the same fractions (result not shown). Both the western blot and Coomassie stained gels provide evidence that the size exclusion chromatography using the 26/60 Sepharose 200 column was unable to separate the proteins and an alternate strategy is required.

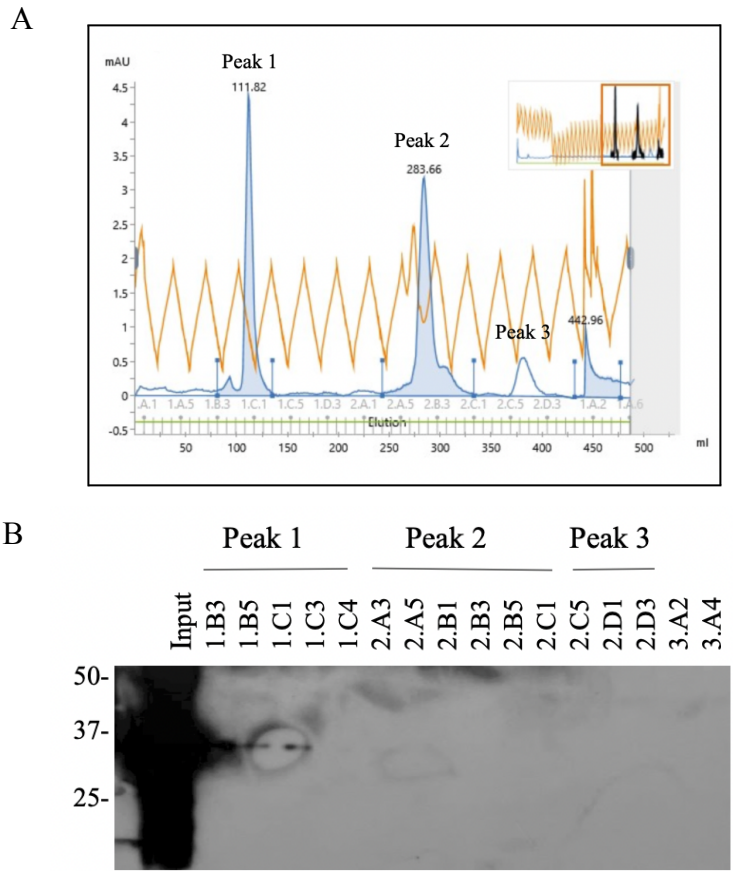

Figure 3.13: (A) Chromatogram shows different UV peaks. (B) Western blot on fractions corresponding to each of the peaks shows that the scFv gets eluted under peak 1 which does not align with the result seen in the previous analytical run. Add coomassie

Ammonium Sulfate precipitation was explored as an alternative to size exclusion chromatography. Several concentrations of ammonium sulfate were tested to find out the optimal conditions for F7-scFv purification and concentration. Western blot and coomassie staining revealed that the F7-scFv can be separated from the contaminant protein by raising the salt concentration to 40%, at which the contaminant gets precipitated leaving the scFv in the supernatant. Furthermore, the F7-scFv can entirely be precipitated at 60% salt saturation and concentrated as desired. This was again confirmed by repeating the experiments only with the above conditions and testing by western blot and coomassie stain. To visualize the protein bands better on the western blot, the 'salted out' samples were desalted using a desalting column.

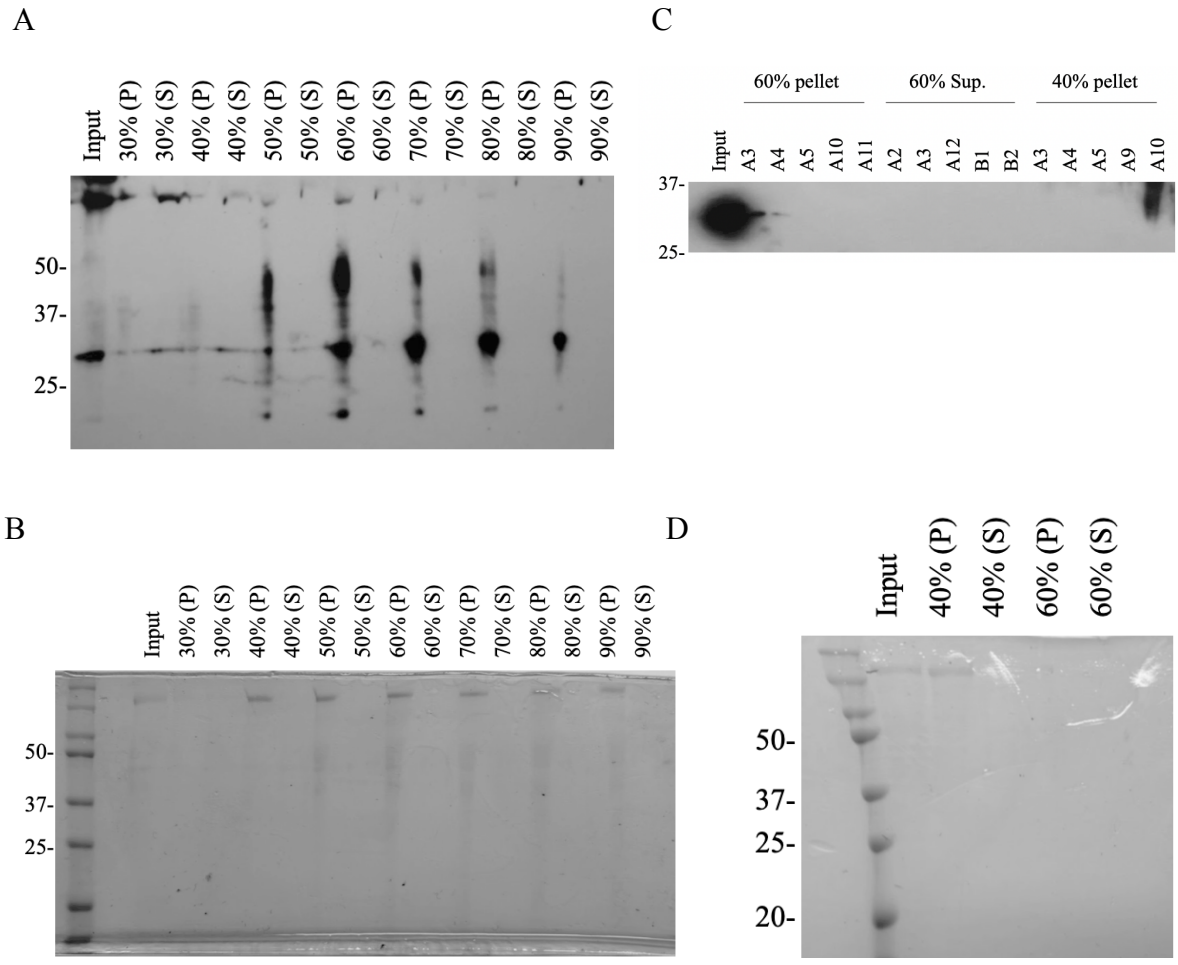

Figure 3.14: (A) Western blot analysis of pellets and supernatants collected from tubes with different amounts of ammonium sulfate shows that the scFv is precipitated almost entirely when salt saturation is raised to 60% or higher. (B) Coomassie staining on the same samples reveals that the large contaminant protein is precipitated at 40% salt saturation or higher as the band is observed at ~ 200 kDa. The western blot(C) and coomassie stained gel (D) of ammonium sulfate precipitated samples further confirmed that 40% and 60% salt saturations can be used to purify and concentrate the scFv respectively. The labeling of the lanes in (C)refers to the particular wells of a 24 deep well plate which was used to collect desalted proteins.

Thus, I tried to remove the contaminant protein from the affinity purified sample using the ammonium sulfate 'salting out' technique. However, the above results could not be replicated likely because of a change in concentration of the saturated ammonium

sulfate solution due to a drop in ambient temperature which may have caused some of the salt to precipitate out (result not shown).

3.3 Binding Studies and Protein Quantification:

3.3.1 Protein G Sepharose Pulldown

The pulldown studies revealed that the Anti-FZD7 scFv successfully binds to its epitope present in the FZD7 ECD-hIgG fusion protein. The negative controls show that the scFv does not non-specifically bind to naked beads.

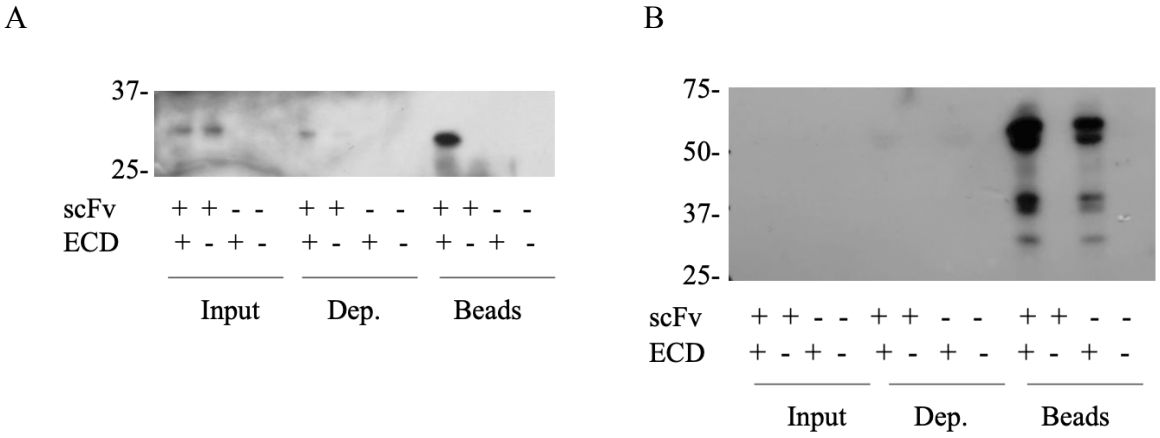

Figure 3.15: (A) The His tagged scFv is enriched in the sample containing ECD and not in the sample without ECD showing that it binds to FZD7 and can be immunoprecipitated using the ECD fusion protein. (B) The Anti-Human secondary HRP blot confirms the presence of ECD in the samples it was added to showing that it was successfully pulled down by the Protein G Sepharose beads.

3.3.2 Indirect ELISA

ELISA was used to study the binding activity of the protein as well as to quantify the amount of protein obtained from each purification step. Chemiluminescent ELISA was used to measure the readout of the reaction. All the steps were followed as described in the methods section with the following changes:1) 96 well white walled plates were used 2)The standards were not used as we only needed to verify scFv binding to FZD7 3)After

incubation with Anti-Human IgG HRP, chemiluminescent reagents (peroxide and luminol) were added in a 1:1 ratio and immediately read using a Promega luminometer. Each condition was performed in triplicates and the averages were taken to plot the graph shown in fig. The graph shows that the highest signal is obtained in the wells containing both FZD7 ECD-hIgG fusion protein and the scFv showing that their interaction is responsible for the readout.

A

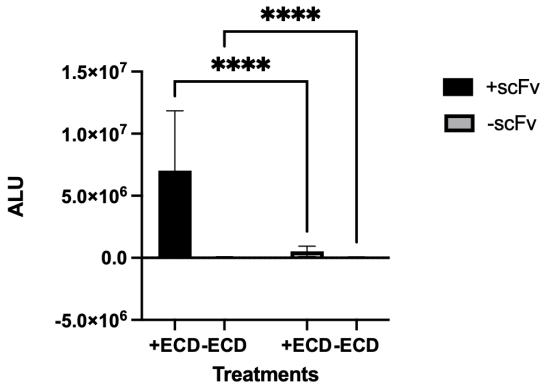

B

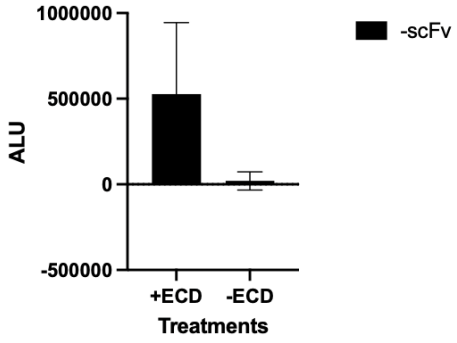

Figure 3.16: The Chemiluminescent ELISA reflects the findings obtained in the ECD pulldown assay. (A) The highest signal is obtained in the wells coated with scFv and treated with ECD which confirms their binding interaction. All other wells containing either of the two proteins produce little to no signal due to the absence of protein-protein interactions. (B) Sample without scFv are replotted to visualize smaller luminescence values.

For protein quantification, the protocol described in section 2.5 (2) was used. A standard curve was plotted and the F7-scFv purified from the 4L affinity run was quantified to be 62.92 ug/ml – 77.46 ug/ml. Further for a total of 20 ml eluted from the affinity run yielded a total protein quantity of 1.25-1.54 mg.

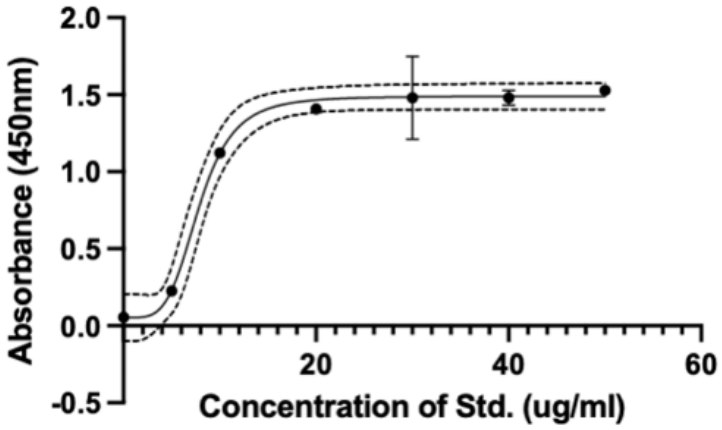

Figure 3.17: Absorbance values of the known standards were modeled using Asymmetric sigmoidal 5PL model on Graphpad Prism.

Table 9: Absorbance values of samples were interpolated onto the graph shown in Figure 3.17 automatically by Prism. Upon multiplying the raw values by their respective dilution factor the concentration of the purified F7-scFv was found to be between 62.92 ug/ml – 77.46 ug/ml. The total amount of protein obtained was found to be 1.25-1.54 mg.

Raw absorbance values of samples	Interpolated Conc. (ug/ml)	Dilution Factor	Final Conc. (ug/ml)
0.11635	3.873	20	77.46
0.45	6.292	10	62.92

3.3.3 Luciferase Assay to see the effect of scFv on WNT signaling:

WNT reporter assay, Super TOP-Flash, revealed that WNT signaling is inhibited by a small degree when cells are treated with the F7-scFv as compared to cells not treated with the F7-scFv. Further, the higher concentration (1:100) of the F7-scFv showed relatively stronger inhibition of WNT signaling than lower concentrations. This effect is also consistent with the WNT + RSPO1 treated cells. This effect is seen presumably due to blocking of WNT binding to FZD7 in the presence of the FZD7 targeting scFv.

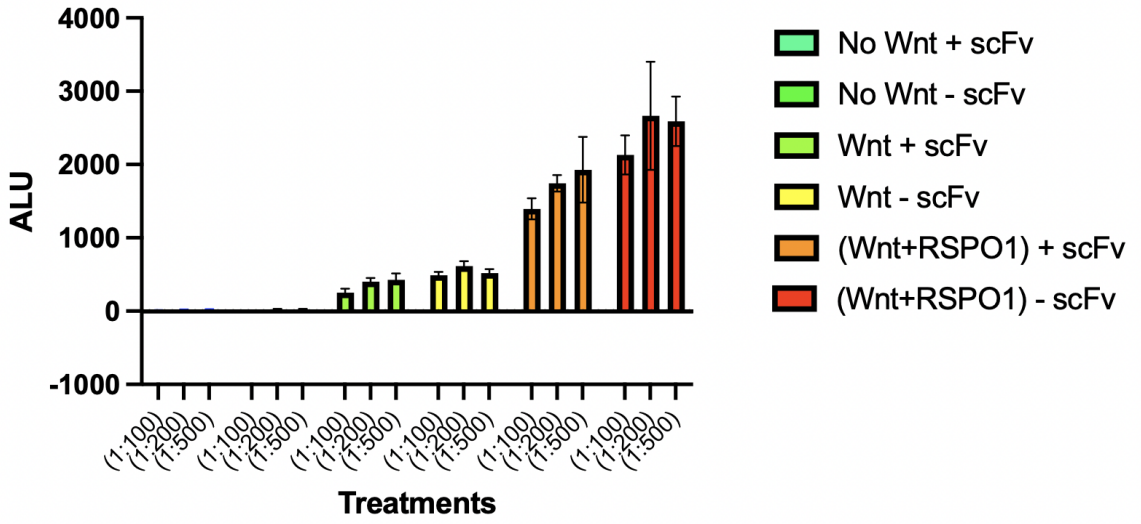

Figure 3.18: WNT signaling is inhibited by a small degree when cells are treated with the scFv.

3.4 Studying Receptor Mediated Targeting of Conjugated LNPs:

Cells treated with 5ug mRNA are shown in figure 3.19. On monitoring for cell death after treatment with LNP-mRNA complex, some cell death was observed at the two highest dosages. However on leaving the cells to incubate overnight, they seemed to recover and grow to confluency. MA148 wild type cells treated with both types of conjugated LNPs showed the presence of a higher number of brighter punctae compared to the FZD7 knockouts. ImageJ quantification also showed that the mean fluorescence of the images of cells treated with the conjugated LNPs was higher than that of the FZD7 knockout cells.

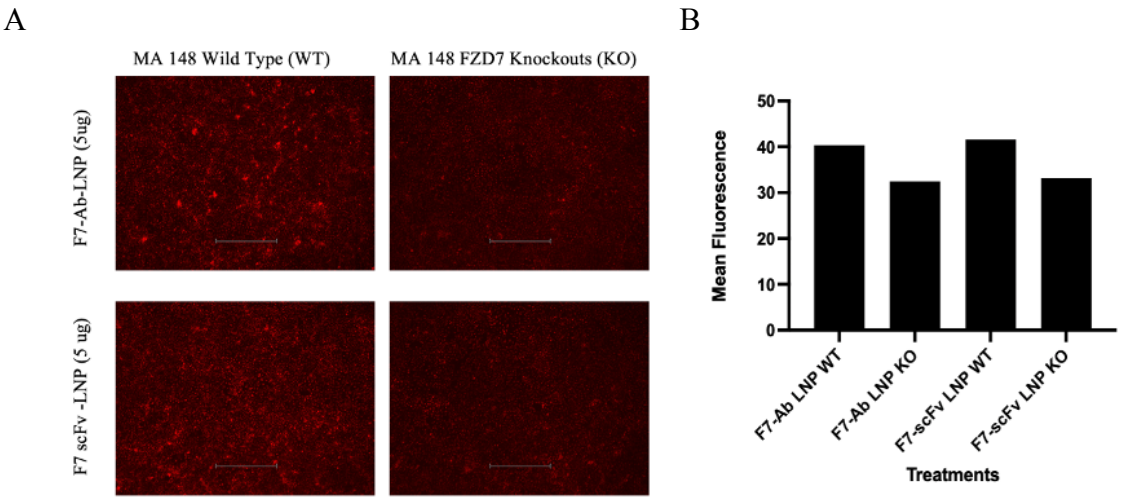

Figure 3.19: (A) MA 148 WT and FZD7 KO treated with 5 ug of mRNA show differential binding of the LNPs to the two cell types. The WT image shows brighter and higher number of red punctae than the FZD7 knockouts indicated FZD7 dependent cell binding. (B) Mean fluorescence of each image calculated by ImageJ also shows higher fluorescence for the WT cells compared to FZD7 KOs for both the conjugated LNPs.

In order to avoid cell death and also assess any nonspecific binding, this assay was repeated using lower dosages of mRNA and adding unconjugated LNP treatment. Cells treated with 1 ug mRNA also showed the same result as above indicating that the LNPs

are bound and/or internalized to cells in FZD7 dependent manner (Figure 3.20). The cells treated with subsequently lower dosages did not show this contrast between the two different cell types.

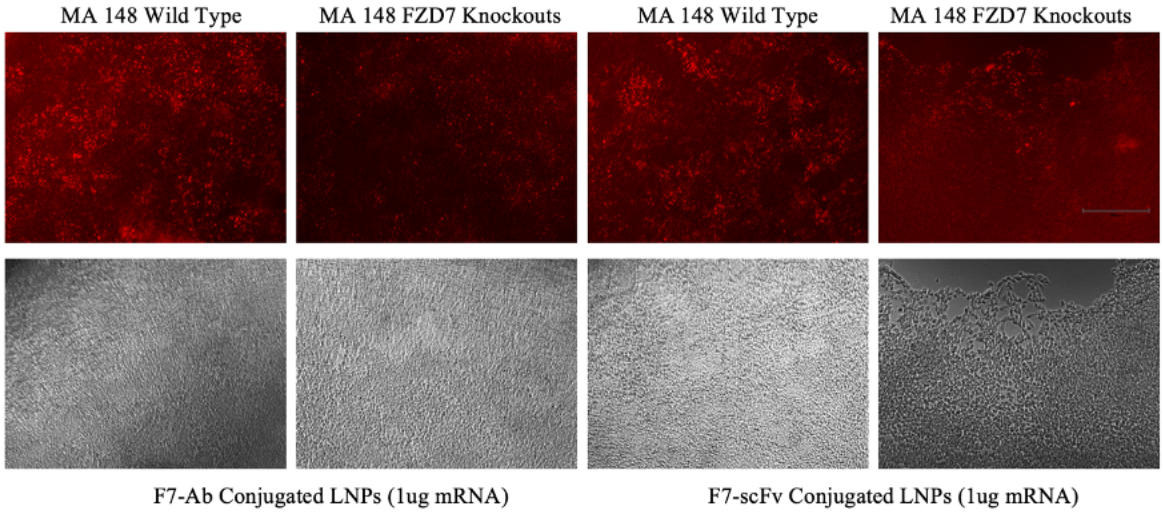

Figure 3.20: MA 148 WT and FZD7 KO treated with a lower dosage of 1 ug of mRNA also show differential binding of the LNPs to the two cell types. The WT image shows brighter and higher number of red punctae than the FZD7 knockouts indicated FZD7 dependent cell binding. Cells were imaged at 10X.

However, when the cells treated with unconjugated LNPs were imaged and observed, the fluorescence was visually and quantitatively similar to the conjugated LNP treated cells indicating that the differential binding to wild type cells is probably not due to the presence of a targeting molecule i.e. the F7-Ab and F7-scFv. This warrants further investigation into the LNP binding, internalization, mRNA release and expression, and the specificity of the targeting molecules.

A B

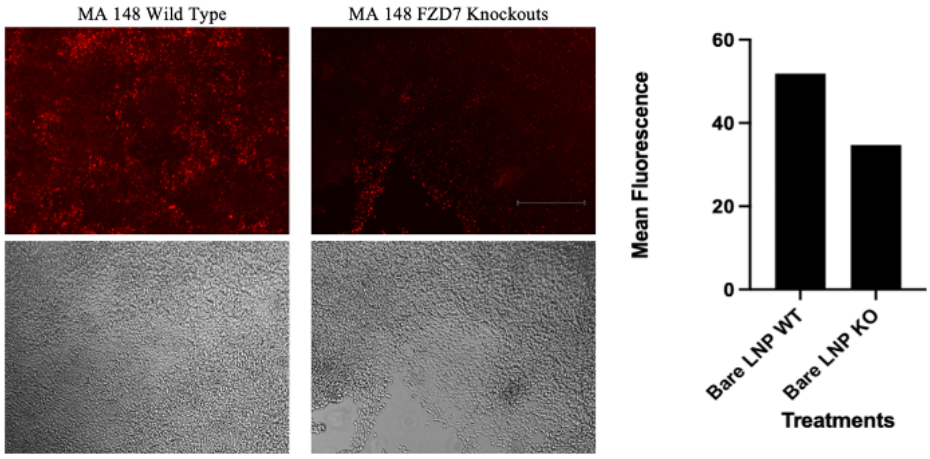

Figure 3.21: Cells treated with unconjugated LNPs were visually and quantitatively similar to the conjugated LNP treated cells indicating that the differential binding to WT cells is probably not due to the presence of a targeting molecule i.e. the F7-Ab and F7-scFv. Cells were imaged at 10X.

CHAPTER 4: CONCLUSIONS AND FUTURE DIRECTIONS

A single chain variable fragment was developed against FZD7 with the purpose of conjugation to LNPs for targeted cancer drug delivery. The scFv was cloned into CHO cells and purified from CHO cell conditioned media using His tag-metal ion affinity chromatography. Further, it was shown that the scFv binds to the FZD7 epitope by co-immunoprecipitation, ELISA and Luciferase assay.

Both the F7-Ab and the F7-scFv were conjugated to LNPs by the Kwon lab and they were tested on MA184 cells for receptor dependent binding. On comparing the Wild Type and FZD7 Knockout cells, FZD7 dependent binding was observed for both types of conjugated LNPs. However, this result needs further investigation as unconjugated LNPs also showed binding to WT cells.

Future experiments may involve observing GFP expression to evaluate FZD7 dependent mRNA expression and nanoparticle tracking analysis to observe each stage i.e. binding, internalization, mRNA release and expression. Further, preclinical studies in murine breast cancer models can be done and tested for tumor regression using cytotoxic drug payloads.

REFERENCES

1) Tepekoy, F., Akkoyunlu, G., & Demir, R. (2015). The role of Wnt signaling members in the uterus and embryo during pre-implantation and implantation. *Journal of assisted reproduction and genetics*, *32*(3), 337–346. https://doi.org/10.1007/s10815-014-0409-7

2) Zhan, T., Rindtorff, N. & Boutros, M. Wnt signaling in cancer. *Oncogene* 36, 1461–1473 (2017). https://doi.org/10.1038/onc.2016.304

3) Nguyen, V. H. L., Hough, R., Bernaudo, S., & Peng, C. (2019). Wnt/β-catenin signalling in ovarian cancer: Insights into its hyperactivation and function in tumorigenesis. *Journal of ovarian research*, *12*(1), 122. https://doi.org/10.1186/s13048-019-0596-z

4) Myan Do, Christina C.N. Wu, Pooja R. Sonavane, Edwin F. Juarez, Stephen R. Adams, Jason Ross, Alessandra Rodriguez y Baena, Charmi Patel, Jill P. Mesirov, Dennis A. Carson, Sunil J. Advani, Karl Willert; A FZD7-specific Antibody–Drug Conjugate Induces Ovarian Tumor Regression in Preclinical Models. *Mol Cancer Ther* 1 January 2022; 21 (1): 113–124. https://doi.org/10.1158/1535-7163.MCT-21-0548

5) Liu, J., Xiao, Q., Xiao, J., Niu, C., Zhang, X., Zhou, Z., Shu, G., Yin, G. Wnt/β-catenin signaling: function, biological mechanisms, and therapeutic opportunities. *Sig Transduct Target Ther* 7, 3 (2022). https://doi.org/10.1038/s41392-021-00762-6

6) Abdulmajeed F. Alrefaei, Frizzled receptors (FZD) play multiple cellular roles in development, in diseases, and as potential therapeutic targets, Journal of King Saud University - Science, Volume 33, Issue 8, 2021, 101613, ISSN 1018-3647, https://doi.org/10.1016/j.jksus.2021.101613

7) Suzuki, M., Kato, C., & Kato, A. (2015). Therapeutic antibodies: their mechanisms of action and the pathological findings they induce in toxicity studies. *Journal of toxicologic pathology*, *28*(3), 133–139. https://doi.org/10.1293/tox.2015-0031

8) Cindy H Chau, Patricia S Steeg, William D Figg, Antibody–drug conjugates for cancer, The Lancet, Volume 394, Issue 10200, 2019, Pages 793-804, ISSN 0140-6736, https://doi.org/10.1016/S0140-6736(19)31774-X.

9) Sadelain, M., Brentjens, R., & Rivière, I. (2013). The basic principles of chimeric antigen receptor design. *Cancer discovery*, *3*(4), 388–398. https://doi.org/10.1158/2159-8290.CD-12-0548

10) Jin, S., Sun, Y., Liang, X. Gu, X., Ning, J., Xu, Y., Chen, S., Pan, L. Emerging new therapeutic antibody derivatives for cancer treatment. *Sig Transduct Target Ther* 7, 39 (2022). https://doi.org/10.1038/s41392-021-00868-x

11) Labrijn, A.F., Janmaat, M.L., Reichert, J.M, Parren, P.W.H.I. Bispecific antibodies: a mechanistic review of the pipeline. *Nat Rev Drug Discov* 18, 585–608 (2019). https://doi.org/10.1038/s41573-019-0028-1

12) Juan, A., Cimas, F. J., Bravo, I., Pandiella, A., Ocaña, A., & Alonso-Moreno, C. (2020). Antibody Conjugation of Nanoparticles as Therapeutics for Breast Cancer Treatment. *International journal of molecular sciences*, *21*(17), 6018. https://doi.org/10.3390/ijms21176018

13) Richards,D. A., Maruani A., Chudasama V (2017) Antibody fragments as nanoparticle targeting ligands: a step in the right direction. *Chemical Science*. https://doi.org/10.1039/C6SC02403C

14) Gumber, D., Do, M., Suresh Kumar, N., Sonavane, P. R., Wu, C. C. N., Cruz, L. S., Grainger, S., Carson, D., Gaasterland, T., & Willert, K. (2020). Selective activation of FZD7 promotes mesendodermal differentiation of human pluripotent stem cells. *eLife*, *9*, e63060. https://doi.org/10.7554/eLife.63060

15) Fernandez, A., Huggins, I. J., Perna, L., Brafman, D., Lu, D., Yao, S., Gaasterland, T., Carson, D. A., & Willert, K. (2014). The WNT receptor FZD7 is required for maintenance of the pluripotent state in human embryonic stem cells. *Proceedings of the National Academy of Sciences of the United States of America*, *111*(4), 1409–1414. https://doi.org/10.1073/pnas.1323697111

16) *ACS Nano* 2021, 15, 11, 16982–17015 Publication Date:June 28, 2021 https://doi.org/10.1021/acsnano.1c04996

17) Waggoner, L., Miyasaki, K., Kwon E.J., (2023). Analysis of PEG-lipid anchor length on lipid nanoparticle pharmacokinetics and activity in a mouse model of traumatic brain injury. *Biomater. Sci.*, 2023,11, 4238-4253. https://doi.org/10.1039/D2BM01846B

18) Wiener, J., Kokotek, D., Rosowski, S. Lickert, H and Meier, M. Preparation of single- and double-oligonucleotide antibody conjugates and their application for protein analytics. *Sci Rep*10, 1457 (2020). https://doi.org/10.1038/s41598-020-58238-6